Whole-genome analyses converge to support the Hemirotifera hypothesis within Syndermata (Gnathifera)

Alexandros Vasilikopoulos[1,*], Holger Herlyn[2], Diego Fontaneto[3], Christopher Gordon Wilson[4], Reuben William Nowell[4,5], Jean-François Flot[6,7], Timothy Giles Barraclough[4], Karine Van Doninck[1,8,*]

[1]Research Unit of Molecular Biology and Evolution, Université libre de Bruxelles (ULB), 1050 Brussels, Belgium
[2]Institute of Organismic and Molecular Evolution (iomE), Anthropology, Johannes Gutenberg University Mainz, 55099 Mainz, Germany
[3]Molecular Ecology Group (MEG), Water Research Institute (IRSA), National Research Council (CNR), 28922 Verbania Pallanza, Italy
[4]Department of Biology, University of Oxford, OX1 3SZ Oxford, UK
[5]Current address: Institute of Ecology and Evolution, University of Edinburgh, EH9 3FL Edinburgh, UK
[6]Evolutionary Biology and Ecology, Université libre de Bruxelles (ULB), Brussels 1050, Belgium
[7]Interuniversity Institute of Bioinformatics in Brussels - (IB)[2], ULB-VUB, 1050 Brussels, Belgium
[8]Research Unit in Environmental and Evolutionary Biology, Université de Namur, 5000 Namur, Belgium

*corresponding authors: A. Vasilikopoulos - email: alexvasilikop@gmail.com, K. Van Doninck - email: Karine.Van.Doninck@ulb.be

Abstract

The clade Syndermata includes the endoparasitic Acanthocephala, the epibiotic Seisonidea and the free-living Bdelloidea and Monogononta. The phylogeny of Syndermata is highly debated, hindering understanding of the evolution of morphological features, reproductive modes and lifestyles within the group. Here, we use publicly available whole-genome data to re-evaluate syndermatan phylogeny and assess the credibility of alternative hypotheses, using a new combination of phylogenomic methods. We found that the Hemirotifera and Pararotatoria hypotheses were recovered under combinations of datasets and methods with reduced possibility of systematic error in concatenation-based analyses. In contrast, the Seisonidea-sister and Lemniscea

hypotheses were recovered under dataset combinations with increased possibility of systematic error. Hemirotifera was further supported by whole-genome microsynteny analyses and species-tree methods that use multi-copy orthogroups after removing distantly related outgroups. Pararotatoria was, nevertheless, only partially supported by microsynteny-based phylogenomic reconstructions. Hence, Hemirotifera, and partially Pararotatoria, were supported by independent phylogenetic methods and data-evaluation approaches. These two hypotheses have important implications for the evolution of syndermatan morphological features, such as the gradual reduction of locomotory ciliation from the common ancestor of Syndermata in the stem lineage of Pararotatoria. Our study illustrates the importance of combining various types of evidence for resolving difficult phylogenetic questions.

Keywords

phylogenomics; outgroup selection; systematic error; synteny; Rotifera; Acanthocephala

Statements and Declarations

Competing interests

The authors declare that they have no competing interests.

Data availability statement

The datasets supporting the conclusions of this article are available in the figshare digital repository (https://figshare.com/s/3c965506085e9817940b; the final link with doi will be provided upon acceptance). Custom bioinformatic scripts that were used for data processing and analysis are also provided on github (https://github.com/alexvasilikop/Rotifer_phylogeny).

Acknowledgements

We thank all members of the Research Unit in Molecular Biology and Evolution (Université libre de Bruxelles, Belgium) and the participants of the XVI International Rotifer Symposium for the interesting and helpful discussions. This work was funded by the Philippe WIENER – Maurice ANSPACH Foundation through a collaborative project of KVD and TGB. This research was also supported by the grant agreement 725998 (RHEA) from the European Research Council (ERC CoG) to K.V.D., providing funding for AV. RWN, CGW and TGB were funded by Natural

Environment Research Council grants NE/M01651X/1 and NE/S010866/1. Financial support by the Deutsche Forschungsgemeinschaft (HE3487/5-1) to HH is gratefully acknowledged.

Introduction

The spiralian clade Syndermata comprises the rotifer clades Bdelloidea, Monogononta, Seisonidea (i.e., the phylum Rotifera *sensu stricto,* composed of free-living species), but also the phylum Acanthocephala, which contains only species with an endoparasitic lifestyle (Fontaneto & De Smet, 2015; Herlyn, 2021). Species of Acanthocephala and Seisonidea are gonochoristic and reproduce sexually with obligate amphimixis (Ricci et al., 1993; Herlyn, 2021), while species of Monogononta are facultative sexual and species of Bdelloidea are obligate asexual (Wallace, 2002; Fontaneto & De Smet, 2015; Terwagne et al., 2022). Therefore, the phylogenetic relationships within Syndermata form an ideal system to test hypotheses on the evolutionary transitions among different lifestyles and reproductive modes (Near, 2002; Herlyn et al., 2003; Min & Park, 2009; Fussmann, 2011). A close evolutionary affinity of Acanthocephala to Rotifera is an old hypothesis based on analyses of both ultrastructural and molecular data (Von Haffner, 1950; Storch & Welsch, 1969; Ahlrichs, 1995, 1997; Winnepenninckx et al., 1995, 1998; Garey et al., 1996; Wallace et al., 1996). From a morphological perspective, the Syndermata hypothesis is strongly supported by the presence of a syncytial epidermis with an intracytoplasmic lamina (e.g., Storch & Welsch, 1969; Ahlrichs, 1995, 1997; Wallace et al., 1996; Zrzavý, 2001; Wallace, 2002; Sørensen et al., 2016). Molecular studies have also provided substantial evidence in support of the Syndermata hypothesis (Winnepenninckx et al., 1995; Garey et al., 1996, 1998; García-Varela & Nadler, 2006; Struck et al., 2014; Wey-Fabrizius et al., 2014; Laumer et al., 2015, 2019). However, the evolutionary relationships among syndermatan subgroups are still highly debated (see Fig. 1a–1f, e.g., Garey et al., 1996, 1998; Melone et al., 1998; Mark Welch, 2000; Sørensen & Giribet, 2006; García-Varela & Nadler, 2006; Witek et al., 2008; Fontaneto & Jondelius, 2011; Lasek-Nesselquist, 2012; Fontaneto, 2014; Wey-Fabrizius et al., 2014; Fontaneto & De Smet, 2015; Sielaff et al., 2016; Mauer et al., 2021). In the present study, we set out to investigate the phylogeny of Syndermata by leveraging publicly available whole-genome data from all major syndermatan subclades and by using a new combination of phylogenomic approaches.

Early molecular phylogenetic studies of Syndermata showed that Acanthocephala is nested within Rotifera *sensu stricto* (Garey et al., 1996, 1998; Winnepenninckx et al., 1998; Mark Welch, 2000; Herlyn et al., 2003; García-Varela & Nadler, 2006; Sørensen & Giribet, 2006), a result that was corroborated later by phylogenomic analyses (Witek et al., 2008; Min & Park, 2009; Wey-Fabrizius et al., 2014; Laumer et al., 2015; Sielaff et al., 2016). A clade Acanthocephala + Bdelloidea (i.e., Lemniscea, Fig. 1b, Lorenzen, 1985) was supported by most of these early molecular phylogenetic studies despite the lack of clear morphological synapomorphies (Clément, 1993; Ricci, 1998). On

the other hand, a sister group relationship of Bdelloidea and Monogononta (i.e., clade Eurotatoria, Fig. 1c) as well as the monophyly of Rotifera *sensu stricto* (Fig. 1f), which were traditionally based on morphological and ecological features (Wallace & Colburn, 1989; Melone et al., 1998), gained little support in the molecular era (Witek et al., 2008, 2009; Min & Park, 2009; Lasek-Nesselquist, 2012). The phylogenetic placement of Seisonidea with respect to the other three groups remained unknown at the dawn of the phylogenomics era, as genomic data from Seisonidea were absent from the first phylogenomic analyses of these groups (e.g., Witek et al., 2008, 2009; Min & Park, 2009; Lasek-Nesselquist, 2012; Hankeln et al., 2014). Despite these observations from molecular studies, according to some researchers there is no strong morphological support against the Eurotatoria and Rotifera hypotheses (Wallace & Colburn, 1989; Melone et al., 1998; Fontaneto & De Smet, 2015).

The absence of typical rotifer characters in species of Acanthocephala is likely due to extreme morphological divergence attributable to their endoparasitic lifestyle (e.g., Mark Welch, 2000, 2005). Additional evidence that acanthocephalans are modified rotifers comes from early studies of ultrastructural data and sperm morphology (Ahlrichs, 1997, 1998; Ferraguti & Melone, 1999), which suggested that Seisonidea and Acanthocephala are sister groups within the syndermatan clade Pararotatoria (Fig. 1a). Later genomic sampling of Seisonidea in phylogenomic analyses further supported the Pararotatoria hypothesis (Wey-Fabrizius et al., 2014; Sielaff et al., 2016; Mauer et al., 2021). Pararotatoria is considered the sister group of Bdelloidea based on the results of the latest phylogenomic studies of Syndermata (Wey-Fabrizius et al., 2014; Sielaff et al., 2016; Mauer et al., 2021). Consequently, Acanthocephala, Bdelloidea and Seisonidea are *ipso facto* placed in a monophyletic group (the Hemirotifera hypothesis, see Fig. 1e, Sørensen & Giribet, 2006; Wey-Fabrizius et al., 2014; Sielaff et al., 2016; Mauer et al., 2021). However, other phylogenomic studies with extensive taxon sampling of Spiralia recovered Seisonidea as sister to all other lineages of Syndermata, suggesting a Seisonidea-sister hypothesis instead of a Monogononta-sister hypothesis (see Fig. 1d, Struck et al., 2014; Laumer et al., 2015). Hence, a reevaluation of the internal phylogeny of Syndermata using new data and methods is needed to test and refine the hypotheses discussed above (Fontaneto, 2014).

Some previous molecular phylogenetic analyses of Syndermata suggested sensitivity of phylogenetic results to the use of distantly related outgroup species, such as flatworm or nematode species (phyla Platyhelminthes and Nematoda respectively, Herlyn et al., 2003; Lasek-Nesselquist, 2012; Mauer et al., 2021). This phenomenon has also been shown to affect phylogenetic analyses of other taxa (Philippe et al., 2009; Li et al., 2012; Pisani et al., 2015). The monotypic phylum

Micrognathozoa, consisting of one described species (*Limnognathia maerski*, see Table 1), is the closest known outgroup of Syndermata (Sørensen et al., 2000, 2016; Sørensen, 2002, 2003; Funch et al., 2005; Laumer et al., 2015, 2019; Marlétaz et al., 2019; Bekkouche & Gąsiorowski, 2022). Bekkouche & Gąsiorowski (2022) suggested the name Gynognathifera for a clade Micrognathozoa + Syndermata. Despite this, no previous phylogenomic study focusing on relationships within Syndermata included data from Micrognathozoa (Wey-Fabrizius et al., 2014; Sielaff et al., 2016; Mauer et al., 2021). More specifically, transcriptomic sampling of Micrognathozoa was only included in a few studies aimed at resolving the phylogenetic position of Micrognathozoa, the phylogeny of Spiralia, or the phylogeny of Metazoa but not specifically the phylogeny of Syndermata (Laumer et al., 2015, 2019; Marlétaz et al., 2019). Since previous phylogenomic studies of Syndermata suggested potential phylogenetic artefacts due to the use of a distantly related outgroup, we reexamined these claims using the more closely related Micrognathozoa as an outgroup.

The phylogeny of Syndermata has also been hypothesized to depend on the taxon sampling of the ingroup, the choice of data for analysis and the choice of evolutionary model (Melone et al., 1998; Min & Park, 2009; Fontaneto & Jondelius, 2011; Lasek-Nesselquist, 2012; Wey-Fabrizius et al., 2014; Sielaff et al., 2016; Mark Welch, 2000; Mauer et al., 2021). It is now well understood that systematic errors can be prevalent in phylogenetic reconstructions based on molecular data across the animal tree of life (Lartillot et al., 2007; Philippe & Roure, 2011; Philippe et al., 2011; Struck et al., 2014). Systematic errors are the result of inadequate evolutionary modelling of the DNA (or amino-acid) substitution process, which is highly heterogeneous (Philippe et al., 2011; Kapli et al., 2020, 2021). The latest molecular studies of syndermatan relationships suggested potential systematic errors affecting the results of the analyses, but they did not employ site-heterogeneous profile mixture models that take into account across-site compositional heterogeneity of the substitution process (Sielaff et al., 2016; Mauer et al., 2021). Other biological processes such as incomplete lineage sorting (ILS) and cross-species gene flow may cause the gene trees to differ from the species tree and can also impede accurate species-tree estimation in concatenation-based analyses (Kubatko & Degnan, 2007; Mendes & Hahn, 2018; Jiao et al., 2020; Kapli et al., 2020; Morel et al., 2022). However, methods that are robust to different biological sources of gene-tree heterogeneity have not been applied to infer the phylogeny of Syndermata. Moreover, many of these methods are now optimized to include multi-copy gene families (or orthogroups) for species-tree estimation, therefore drastically increasing the total number of genes for analysis (Smith & Hahn, 2021). This allows us to reexamine the validity of previous phylogenetic results of

syndermatan relationships using independent methods that account for different sources of heterogeneity in the data. Additionally, whole-genome data are now available for all syndermatan subgroups, making it possible to investigate the phylogeny of Syndermata using whole-genome structural data (e.g., Drillon et al., 2020; Schultz et al., 2023; Zhao et al., 2021). Such whole-genome structural approaches are less likely to be sensitive to homoplasy and substitution saturation than conventional sequence-based approaches and complement the results of the sequenced-based analyses (Niehuis et al., 2012; Lehmann et al., 2013; Sielaff et al., 2016; Cloutier et al., 2019; Ontano et al., 2021; Schultz et al., 2023; Zhao et al., 2021; Parey et al., 2023). Congruent findings from different methods and datasets should ideally be the aim of modern phylogenomic studies (Tihelka et al., 2021; Vasilikopoulos et al., 2021b). Despite this, the congruence of syndermatan phylogenetic relationships across different analyses has yet to be tested using results from these new genome-scale structural and gene-tree-based phylogenomic approaches.

In this study, we reexamine the phylogenetic relationships within Syndermata using a new combination of phylogenomic approaches, namely: 1) concatenation-based analyses using profile mixture models that account for long-branch attraction artefacts due to compositional heterogeneity across sites, 2) species-tree methods that utilize multi-copy orthogroups for phylogenetic inference and 3) whole-genome microsynteny-based phylogenomic analyses of syndermatan relationships. Our main aim was to test congruence among different methods and datasets concerning some previously suggested phylogenetic relationships of Syndermata (Fig. 1), and also to discuss the different approaches while taking into account previous morphological analyses.

Methods

Taxon sampling and processing of genomic and transcriptomic datasets

We used 11 published genomes (Syndermata: 9, Platyhelminthes: 2) and one published transcriptome, belonging to the micrognathozoan species *L. maerski*, to address the phylogenetic relationships of Syndermata (Table 1, Online Resource 1: Fig. S1, Laumer et al., 2015; Nowell et al., 2018, 2021; Mauer et al., 2020, 2021; Kim et al., 2021; Simion et al., 2021). Gene annotations were downloaded from the NCBI, WormBase Parasite v. 17.0 and PlanMine v. 3.0 databases (see Table 1 and Online Resource 1, Howe et al., 2017; Rozanski et al., 2019). Gene predictions for the genome of *Proales similis* were performed using Funannotate v. 1.8.11 (see Online Resource 1 for details). All gene-annotation GFF files and corresponding FASTA files were then processed with custom python scripts to remove pseudogenes, alternative transcripts or isoforms, and tRNA genes before orthology prediction. The filtered gene annotations and corresponding FASTA files are

provided in the supplementary files (see data availability section). Transcriptomic reads for *L. maerski* were downloaded from the NCBI-SRA database and were subsequently trimmed and assembled with Trinity v. 2.14.0 (see Online Resource 1, Grabherr et al., 2011). The assembled transcripts were then used as input for TransDecoder v. 5.5.0 to predict a credible set of protein sequences for downstream analyses (see Online Resource 1 and Table 1). Gene completeness of protein datasets was inferred using universal single-copy orthologs (BUSCO) v. 5.2.2 (Manni et al., 2021, Table 1, Online Resource 1: Fig. S1).

Orthology prediction, single-copy ortholog set construction and supermatrix generation

Orthology prediction using the 12 species' proteomes was performed with Orthofinder v. 2.5.4 with the options: -M msa -T raxml-ng (Emms & Kelly, 2019; Kozlov et al., 2019). The results of orthology prediction showed that only 101 orthogroups (OGs) contained single-copy genes across all species. This could be partially due to the whole-genome duplication event in the stem lineage of bdelloid rotifers (Mark Welch et al., 2008; Hur et al., 2009), which could place bdelloid-specific gene duplications (i.e., homoeologs) in the same OG. The presence of uncollapsed haplotypes in genome assemblies or the overall low total number of genes in the genomes of *Proales similis* (Monogononta), *Seison nebaliae* (Seisonidea) and *Pomphorhynchus laevis* (Acanthocephala) could be additional reasons. To increase the total number of genes for phylogenomic analyses, we therefore proceeded by inferring different sets of single-copy orthogroups (SCOGs) using different methodological approaches, starting from the initial OGs inferred by Orthofinder (see Table 2, Online Resource 1: Fig. S2–S4). In the first approach, we selected SCOGs that included at least 10 out of the 12 species to create supermatrix A (Table 2, Online Resource 1: Fig. S2). In the second approach, we first selected SCOGs that contained at least one species from each of the six taxonomic groups whose phylogenetic relationships we wanted to address (Acanthocephala, Bdelloidea, Monogononta, Seisonidea, Micrognathozoa, Platyhelminthes). This set of genes is called taxonomically "decisive" and contained 177 SCOGs (Dell'Ampio et al., 2014). We subsequently added to this set all decisive multi-copy OGs with species-specific gene multiplications after keeping only one copy per species (see supermatrix B, only OGs with multiple copies in only one non-bdelloid species were considered at this step, see Table 2 and Online Resource 1: Fig. S2). In the third approach we used orthoSNAP v. 0.1.1 to identify SCOGs within larger multi-copy OGs (min. number of species required for each SCOGs: 10, supermatrix C, Table 2, Online Resource 1: Fig. S2, see Steenwyk et al., 2022). Lastly, we inferred one set of SCOGs to account for the ancient whole-genome duplication event in bdelloid rotifers (Mark Welch et al., 2008; Hur et al., 2009). Specifically, we first selected taxonomically decisive OGs that had multiple

gene copies only in one or more bdelloid species (Online Resource 1: Fig. S2). The subtrees of bdelloid sequences were then extracted from the pre-inferred OG trees of Orthofinder using ETE v. 3.1.2 (Huerta-Cepas et al., 2016). We then searched for SCOGs within the extracted bdelloid subtrees using the same version of orthoSNAP as above (min. number of species required: 4). The bdelloid sequences of the extracted SCOGs were then combined with the single-copy sequences of non-bdelloid species in the same OG (see supermatrix D, Table 2, Online Resource 1: Fig. S2). By using these semi-independent approaches to SCOG selection, we reduced the possibility of biased phylogenetic estimates due to hidden paralogy in some SCOG sets (Emms & Kelly, 2019; Siu-Ting et al., 2019). The custom python scripts that were used for generating the different ortholog sets from the output of Orthofinder are provided on github (see data availability section).

Supermatrices were assembled and analyzed only at the amino-acid sequence level. Before inferring multiple sequence alignments (MSAs), we used PREQUAL v. 1.02 to screen each of the previously inferred SCOGs and mask potentially non-homologous and erroneous amino-acid sequence segments (Whelan et al., 2018). This type of segment filtering has been shown to improve branch-length estimation in molecular phylogenetics (Di Franco et al., 2019), and is relevant for inferring an accurate phylogenetic tree of Syndermata that is often characterized by high levels of branch-length heterogeneity (e.g., Struck et al., 2014; Laumer et al., 2015). Amino-acid sequences in each SCOG were aligned using the software FSA v. 1.15.9 (option: --fast) that greatly reduces false positive alignments and therefore increases the overall accuracy of MSAs (Bradley et al., 2009). We subsequently used BMGE v. 1.12 (options: -h 0.5 -m BLOSUM62) to remove hypervariable alignment columns from the individual MSAs (Criscuolo & Gribaldo, 2010; Vasilikopoulos et al., 2021a). The filtered MSAs of the different sets of SCOGs were then concatenated into four different supermatrices using PhyKIT v. 1.11.7 (supermatrices A, B, C, and D in Table 2 and Online Resource 1: Fig. S2; Steenwyk et al., 2021). We also analyzed the original supermatrix generated by Orthofinder after trimming it with the same version of BMGE as described above (see Table 2, supermatrix E). This supermatrix is constructed internally by Orthofinder after selecting OGs for which at least 66% of the species in the dataset are single-copy (Emms & Kelly, 2019).

Selecting subsets of genes, alignment sites and species for downstream sensitivity analyses

Several approaches have been used to select optimal subsets of genes and sites for phylogenomic analyses that rely on different criteria (Misof et al., 2013; Salichos & Rokas, 2013; Klopfstein et al., 2017; Naser-Khdour et al., 2019; McCarthy et al., 2023). We applied genesortR (version 12.10.2022) on supermatrices A, B, C and D to select subsets of the 50 most reliable loci from each

supermatrix (supermatrices A50.1, B50.1, C50.1 and D50.1, Mongiardino Koch, 2021). GenesortR performs multivariate analyses of several gene properties and attempts to find a PCA axis of usefulness along which proxies for phylogenetic signal increase whereas proxies for systematic bias decrease. GenesortR requires a species tree as input for estimating Robinson-Foulds distances of gene trees to the species tree. This distance is used as a proxy for phylogenetic signal of the genes. However, this presupposes that the species tree is known *a priori*. To avoid selecting genes that favor a specific topology of syndermatan relationships, we used a tree topology for which the relationships of the major syndermatan groups were collapsed into a polytomy. Individual gene trees for each SCOG were estimated independently and were then provided to the genesortR script (see Online Resource 1).

Since outgroup selection was previously shown to affect phylogenetic inference of Syndermata, we also tested whether removing the two distantly related species of Platyhelminthes affected the inferred syndermatan relationships. Specifically, we removed the two flatworm species from supermatrices A50.1, B50.1, C50.1 and D50.1 and E to generate five additional supermatrices that contained *L. maerski* as the outgroup (Fig. 1a, Table 2, supermatrices: A50.2, B50.2, C50.2, D.50.2, F). Moreover, since we observed extreme branch-length heterogeneity within Syndermata and possible heterogeneous sequence divergence for the acanthocephalan species *P. laevis* (Figs. 1d, 1e, see below for results of the AliGROOVE analysis), we subsequently applied an alignment-site removal strategy to homogenize branch lengths within the ingroup, generating supermatrices A50.3, B50.3, C50.3, D.50.3, H (Fig. 1a, Table 2). This is because previous studies have shown that selecting a closely related outgroup should be accompanied by taking into account properties of the ingroup and outgroup taxa as well (Borowiec et al., 2019; Vasilikopoulos et al., 2021a). Because the inclusion of Platyhelminthes in phylogenetic analyses seemed to have had an impact on the internal topology of Syndermata, we only applied this site-removal strategy to supermatrices from which the two species of Platyhelminthes had been previously removed (Fig. 1a, Table 2, supermatrices A50.2, B50.2, C50.2, D.50.2, F). To be more specific, we deleted alignment columns with unique amino-acid residues for *Seison nebaliae* (Seisonidea), *Pomphorhynchus laevis* (Acanthocephala) or for both species from these supermatrices using custom python scripts. Alignment columns were not removed if additional species in the same column also had a unique amino-acid to avoid eliminating too many informative sites. Using supermatrix F (that was larger in terms of alignment positions) as input, we also performed two additional filterings: (1) by deleting all columns that included any number of unique amino-acid residues (supermatrix G), and (2) by deleting columns with unique amino-acid residues in only 1 of all the species in the alignment (supermatrix I).

Measuring data completeness, deviation from compositional homogeneity and other statistical properties of amino-acid supermatrices

Most commonly used models of molecular evolution assume that sequences have evolved under stationary, homogeneous and reversible conditions (SRH, Ababneh et al., 2006; Jermiin et al., 2008). If the data violate these assumptions there is an increased chance for erroneous phylogenetic estimates using these models (Ababneh et al., 2006; Jermiin et al., 2008; Naser-Khdour et al., 2019). To measure the degree of deviation from compositional homogeneity among species in each analyzed supermatrix, we inferred relative composition frequency variability values (RCFV, Online Resource 2: Table S1) with BaCoCa v. 1.109 (Zhong et al., 2011; Kück & Struck, 2014). Complementary to the RCFV approach, we performed the matched-pairs tests of homogeneity for all supermatrices using the Bowker's symmetry test (Bowker, 1948; Ababneh et al., 2006). Matched-pairs tests of symmetry were performed with Homo v. 2.0 (available from: https://github.com/lsjermiin/Homo.v2.0, last access 16.11.2022) and heatmaps of pairwise symmetry tests were generated with HomoHeatmapper v. 1.0 (available from: https://github.com/lsjermiin/HomoHeatMapper, last access 16.11.2022, see Jermiin et al., 2020).

We additionally inferred completeness scores for all supermatrices, heatmaps of pairwise completeness scores and average pairwise *p*-distances using AliStat v. 1.14 (Wong et al., 2020). Lastly, we inferred substitution saturation scores (Philippe et al., 2011), the standard deviation of long-branch scores (LB score standard deviation, Online Resource 2: Table S1, Struck, 2014), and treeness-over-RCV scores (treeness divided by relative composition variability, TORCV, Online Resource 2: Table S2) using the same version of PhyKIT as above (Phillips & Penny, 2003; Steenwyk et al., 2021). Treeness (or 'stemminess') of a phylogenetic tree measures the proportion of tree distance on the internal tree branches and can be used as a measure of the signal-to-noise ratio in a phylogeny (Lanyon, 1988; Phillips & Penny, 2003; Steenwyk et al., 2021). Relative composition variability (RCV) measures the amino-acid (or nucleotide) composition variability across species in the underlying MSA (Phillips & Penny, 2003). Higher TORCV scores are therefore desirable, as they are associated with higher signal-to-noise ratio and reduced compositional and other biases (Phillips & Penny, 2003; Steenwyk et al., 2021). The LB score measures for each species the percentage deviation from the average patristic distance across all pairs of species and is a metric that is independent of the root of the tree (Struck, 2014). The standard deviation of LB scores of a phylogenetic tree provides a measure of branch-length heterogeneity (Struck, 2014). Lower standard deviation of LB scores is associated with reduced

branch-length heterogeneity and thus reduced potential for long-branch attraction (Struck, 2014). We used the maximum-likelihood trees with the best log-likelihood scores that were inferred under the best-fitting models (see following section) for inferring all tree-dependent statistics for each supermatrix (i.e., saturation scores, standard deviation of LB scores, TORCV values, see Online Resource 2: Table S1). Lastly, we also screened the supermatrices with reduced taxon sampling for evidence of heterogeneous sequence divergence of individual species with AliGROOVE v. 1.08 (Kück et al., 2014). AliGROOVE maps suspicious branches on a phylogenetic tree based on the pairwise similarity of sequences in the MSA can help identify highly divergent or saturated sequences. Such sequences are often characterized by extremely long branches in inferred phylogenetic trees and might be incorrectly placed in a phylogeny (Kück et al., 2014). Processing and analysis of the properties of supermatrices and species was performed with pandas v. 1.4.3, while statistical visualization of these properties was performed using matplotlib v. 3.5.1 and seaborn v. 0.11.2 (Hunter, 2007; McKinney, 2010; Waskom, 2021).

Model selection and phylogenetic reconstruction with site-heterogeneous and site-homogeneous substitution models

Phylogenetic reconstructions were performed both in maximum-likelihood and Bayesian frameworks. For maximum-likelihood analysis, we first selected the best-fit substitution model for phylogenetic reconstruction with ModelFinder as implemented in IQ-TREE v. 1.6.12 (Nguyen et al., 2015; Kalyaanamoorthy et al., 2017). Our model selection procedure was performed on unpartitioned supermatrices by including empirical profile mixture models with 61 components (C60+F models) that account for among-site compositional heterogeneity (i.e., site-heterogeneous, see Online Resource 1, Le et al., 2008). In total 70 models were tested on each supermatrix. Phylogenetic tree reconstructions were performed with the best-fit substitution model for each supermatrix and the same version of IQ-TREE. Since site-heterogeneous models always had a better fit than site-homogeneous models, we also analyzed all supermatrices with the site-homogeneous LG+F+R5 model to test the sensitivity of phylogenetic results to model miss-specification. We performed five independent tree searches with 1) the best-fit model and 2) with the LG+F+R5 model and selected the tree with the best log-likelihood score among the five tree searches as the best maximum-likelihood tree under each model to avoid potential local optima in the analyses (Stamatakis & Kozlov, 2020). IQ-TREE produced a warning that the mixture models might be overfitting because a few mixture weights were estimated close to 0 (despite being selected as the best models). For this reason, we repeated the tree searches for all supermatrices with a less complex site-heterogeneous profile mixture model (e.g., LG+C20+F+R5, see Online

Resource 2: Table S2) and compared results of phylogenetic reconstructions. Statistical branch support was estimated based on 1000 ultrafast bootstrap replicates (UFB, with the option -bnni to avoid inflated branch support due to inadequate modelling) and 2000 SH-aLRT replicates in all cases (Guindon et al., 2010; Hoang et al., 2018).

We also performed Bayesian phylogenetic inference of Syndermata relationships for a selection of supermatrices with the site-heterogeneous CAT+GTR+G4 model as implemented in phylobayes-mpi v. 1.9 (see Online Resource 2: Table S2, Lartillot & Philippe, 2004; Lartillot et al., 2013; Lartillot, 2020). Two independent Markov chain Monte Carlo (MCMC) analyses were run for each analyzed supermatrix until convergence. Convergence in the tree space was assessed with bpcomp (maxdiff < 0.1, default parameters), and we also checked for convergence of the parameter values with tracecomp (a run with an effective size > 50 for all parameters is considered acceptable according to the manual of phylobayes). Posterior consensus trees using two chains for each analyzed supermatrix were then produced with bpcomp (Lartillot, 2020). All inferred phylogenetic trees were rooted and visualized with iTOL v. 6 (Letunic & Bork, 2021). Lastly, we performed posterior predictive tests, in order to check for adequacy of the GAT+GTR+G4 model to describe 1) across-species compositional heterogeneity and 2) specificity of amino-acid compositions of sites due to biochemical constraints in the supermatrices (Bollback, 2002; Feuda et al., 2017; Lartillot 2020). Using these tests, we also monitored the effect of distant outgroup removal on the ability of the model to describe compositional patterns across species and sites in the supermatrices. Posterior predictive tests for (a) compositional heterogeneity across species (two summary statistics used: (a) maximum and (b) mean squared heterogeneity, option: -comp), and (b) mean site-specific amino acid diversity (option: -div) were performed using the same version of phylobayes. For performing these posterior predictive tests, we simulated at least 100 datasets from the posterior distribution for supermatrices A50.1, A50.2, B50.1, B50.2, B50.3, C50.1, C50.2, D50.1, D50.2. D50.3 (Online Resource 2: Table S3).

Comparing properties of supermatrices that support or not the different syndermatan relationships

Since the above-described removal of sites with unique amino acids resulted in improved values concerning statistical properties with putative connection to systematic error (i.e., LB score standard deviation, TORCV), and because not all analyses of filtered datasets resulted in the same syndermatan topology (Fig. 2b), we assessed the plausibility of four hypotheses of syndermatan relationships by evaluating under which conditions each of these hypotheses (or clades) is inferred or not inferred (Fig. 2b, Fig. 3a-3d). The hypotheses that we tested are: 1) monophyly of

Acanthocephala + Bdelloidea + Monogononta (i.e., the Seisonidea-sister hypothesis), 2) Acanthocephala is the sister group of Bdelloidea (the Lemniscea hypothesis), 3) monophyly of Acanthocephala + Bdelloidea + Seisonidea (the Hemirotifera or Monogononta-sister hypothesis), 4) Acanthocephala is the sister group of Seisonidea (the Pararotatoria hypothesis, see Figs. 2b, 3a-3d). We selected these hypotheses based on the results of previous molecular phylogenetic studies but also based on the results of our own analyses. Note that not all tested hypotheses are mutually exclusive, as the Hemirotifera hypothesis is compatible with both the Pararotatoria and the Lemniscea hypothesis. On the other hand, the Seisonidea-sister hypothesis is only compatible with the Lemniscea hypothesis.

Assuming sufficient phylogenetic signal given the size of our supermatrices (> 12,000 amino-acid sites, Table 2), we postulated that inference or not of each these hypotheses is likely due to systematic error in concatenation-based analyses (i.e., inability of the model to accommodate some heterogeneity in the evolutionary process). We further postulated that dataset properties with potential connection systematic error (i.e., TORCV, standard deviation of LB scores and saturation scores) could be used to evaluate datasets as more or less likely to produce trees influenced by systematic error. More specifically, if datasets supporting a phylogenetic hypothesis have more desirable properties (i.e., higher TORCV, lower standard deviation of LB scores and higher saturation scores) than datasets that do not support it, then it is less likely that this hypothesis is artefactual. In contrast, if their properties are less desirable than the properties of datasets that do not support a hypothesis, then this hypothesis should be considered less likely. We plotted the median: 1) TORCV score, 2) standard deviation of LB scores and 3) saturation score separately for: (a) the datasets that supported and (b) the datasets that did not support each of these four hypotheses (Fig. 3a-d). These analyses were only performed based on datasets for which species of Platyhelminthes had been removed (supermatrices: F, G, H, I, A50.2, A50.3, B50.2, B50.3, C50.2, C50.3, D50.2, D50.3). Analyses were repeated after excluding the results of supermatrix G, as this was the most stringently trimmed supermatrix, showing extreme values of standard deviation of LB scores (low), TORCV (high), and saturation score (low, Online Resource 1: Fig. S5).

Species-tree inference from multi-copy orthogroups

As an alternative approach to the concatenation-based analyses, we applied phylogenomic methods that leverage information from both single- and multi-copy gene families (or OGs). We applied different species-tree methods that take into account different biological sources of gene-tree heterogeneity (Maddison, 1997). First, we selected taxonomically decisive OGs that contained a

maximum of five gene copies per species (2,010 OGs, Online Resource 1: Fig. S2). Subsequently, we used the gene trees of these OGs (inferred internally by Orthofinder) for species-tree reconstruction with SpeciesRax that is part of the software package GeneRax v. 2.0.4 (Morel et al., 2020, 2022). SpeciesRax is robust to differential gene duplication and loss but also gene transfer events when inferring a species tree from a set of multi-and single-copy gene trees. We also applied ASTRAL-Pro v. 1.10.1.3 on the same set of gene trees (Zhang & Mirarab, 2022). ASTRAL-Pro has been shown to be statistically consistent under the multi-species coalescent model and can therefore compensate for incomplete lineage sorting (Zhang et al., 2020; Zhang & Mirarab, 2022). Lastly, we applied the species-tree inference method that is implemented in STAG v. 1.0.0 (Emms & Kelly, 2018). STAG computes the shortest inter-species distances in the individual OG trees to construct distance matrices and species trees for each OG and therefore takes into account only OGs that include at least one gene copy from each species in the dataset. This collection of preinferred species trees is then used to infer a greedy consensus species tree from all OGs that contain all species (Emms & Kelly, 2018, 2019). Since the STAG method can only process OGs that contain all species in the putative species tree, the number of OGs was reduced from 2,010 to 1,479 for the initial STAG analysis. When the two species of Platyhelminthes were removed from the initial 2,010 OGs, the number of informative OGs was reduced from 2010 to 1628 for the same analysis.

Since individual OG trees were inferred by default using the LG+G4 model within the Orthofinder pipeline, we tested whether selecting the best-fit model for inferring the OG trees affected the downstream species-tree inference. We selected the best-fit substitution model for each OG using the Orthofinder MSAs and IQ-TREE v. 1.6.12 (AICc criterion, see Online Resource 1 for detailed commands). Phylogenetic tree reconstruction for each preinferred MSA was then performed with the same version of IQ-TREE. Species-tree reconstructions were subsequently repeated using the same versions of GeneRax, ASTRAL-Pro, and STAG as above. Using the OG trees that were inferred with the best-fit models, we also selected and analyzed subsets of the best OG trees with 1) increased signal-to-noise ratio and reduced compositional bias (highest TORCV scores) and 2) reduced branch-length heterogeneity (lowest standard deviation of LB scores). For each of the two subsampling strategies, we analyzed a) the top 50% (1005 of 2010) and b) the top 500 genes. TORCV values and LB standard deviation scores for each gene tree were calculated with the same version of PhyKIT as described above. Because of previous claims that the internal phylogeny of Syndermata is negatively affected by using a distantly related outgroup, we also checked whether removing all sequences of Platyhelminthes from the OGs affected the phylogenetic results of species-tree methods. For doing this, we removed the two species of Platyhelminthes from all

previously selected MSAs of OGs, re-inferred gene trees and repeated all species-tree reconstructions as described above.

Microsynteny-based phylogenetic reconstruction of Syndermata

As a last approach to species-tree inference, we performed microsynteny-based phylogenetic reconstructions with the software package syntenet v. 1.0.2 using R v. 4.2.2 (R Core Team, 2021; Almeida-Silva et al., 2023). For this analysis we used as input the GFF and proteome files of all genomes in our dataset (all species except *L. maerski*, see Table 1). First, all-versus-all BLASTp searches for the input proteomes were performed with DIAMOND v. 2.0.13.151 within the syntenet R package (Buchfink et al., 2021). The BLAST results and the genomic coordinates of genes were automatically used to infer synteny network across all genomes using a version of MCScanX that is implemented within syntenet (Wang et al., 2012; Almeida-Silva et al., 2023). We used three different combinations of parameters for defining syntenic blocks and repeated all phylogenetic analyses below for each parameter combination: (a) max_gaps = 60 and anchors = 2, (b) max_gaps = 60 and anchors = 3, (c) max_gaps = 80 and anchors = 2. These relaxed parameters for identifying syntenic blocks were used because it was previously shown that the microsynteny approach might work better with more permissive synteny parameters in distantly related taxa (Zhao et al., 2021), and because the genomes of Syndermata showed reduced levels of deeply conserved synteny. Subsequently, we performed clustering of the synteny network and performed phylogenomic profiling of the clusters to identify which of them are present in which phylogenetic groups using the provided functions within the package syntenet. Absence or presence of the inferred synteny clusters across species was then used to perform microsynteny-based species-tree reconstruction. Specifically, the phylogenomic profiles across species were converted to a supermatrix of binary characters (0, 1) for phylogenetic analysis. A different supermatrix was produced for each set of synteny-block definition parameters. The binary data were treated as discrete morphological characters for phylogeny estimation in a maximum-likelihood framework (option: -st MORPH in IQ-TREE). Best-fit substitution models for the binary-data supermatrices were selected using default options in ModelFinder (option: -m MFP) and phylogenetic trees were inferred using IQ-TREE v. 1.6.12. Statistical branch support was assessed with 1000 UFBs (option: -bnni) and 2000 SH-aLRT replicates. The phylogenetic trees were rooted and visualized with iTOL v. 6 after omitting branch lengths in order to show only the species-tree topology (Letunic & Bork, 2021). Our microsynteny-based phylogenetic approach did not include *L. maerski*, as whole-genome data were not available for this species.

We also used site-concordance factors to estimate discordance of phylogenomic signal in the microsynteny data with respect to the two competing hypotheses of early syndermatan relationships (Monogononta-sister vs. Seisonidea-sister hypotheses, Minh et al., 2020a; Mo et al., 2023). The site-concordance factor is defined as the percentage of decisive alignment sites (i.e., in this case microsynteny clusters) supporting a branch in the reference tree (averaged over all quartets around this branch). We estimated site-concordance factors using both parsimony and maximum likelihood methods (SCF and SCFL respectively, Minh et al., 2020a; Mo et al., 2023) and by using all possible quartets. Site-concordance factors for the Monogononta-sister (i.e., Hemirotifera) hypothesis were inferred by providing the preinferred species-tree topologies to IQ-TREE. Calculation of site-concordance factors in support of the Seisonidea-sister hypothesis (i.e., a clade Bdelloidea + Monogononta +Acanthocephala) was performed by supplying a fixed tree topology to IQ-TREE for which *Seison nebaliae* was placed as sister to all other syndermatan species, leaving the rest of phylogenetic relationships unchanged. All site-concordance factor analyses were performed with IQ-TREE v. 2.2.2 (Minh et al., 2020b).

Results

Orthology prediction and ortholog-set selection

The orthology prediction analysis with Orthofinder resulted in a total number of 273,614 genes from 12 species being assigned to 31,139 OGs (~90.5 % of genes were assigned to OGs). A total of 8,594 OGs were species-specific (i.e., contained genes of only one species). In contrast, 28,832 genes were not assigned to any OG (~9.5 % of genes). The Orthofinder analysis also produced a set of 101 SCOGs, each composed of single-copy genes from every species in the analysis. Since this number of SCOGs was considered relatively low for phylogenetic analysis we did not directly use this set of SCOGs for downstream phylogenomic inference. However, extracting all SCOGs that contained at least 10 out of 12 species from the output of Orthofinder resulted in an increased number of SCOGs (n = 345, supermatrix A, Fig. 2a, Table 2, Online Resource 1: Fig. S2).

Using the output of Orthofinder, we additionally identified 2,010 decisive OGs that contained at least one species from each focal taxonomic group (Acanthocephala, Bdelloidea, Monogononta, Seisonidea, Micrognathozoa, Platyhelminthes) and maximum five gene copies per species (Online Resource 1: Fig. S2). Starting from this set of OGs, the remaining sets of SCOGs were inferred (i.e., ortholog sets). These sets were the basis for assembling supermatrices B, C and D (Online Resource 1: Figs S1–S4). More specifically, combining (a) decisive SCOGs (i.e., with >= 1 species from each taxonomic group) with (b) decisive OGs that had species-specific gene multiplications in only one

non-bdelloid species resulted in 233 SCOGs (ortholog set of supermatrix B, Fig. 1a, Table 2, Online Resource 1: Fig. S2). The orthoSNAP analysis resulted in 267 single-copy subgroups of OGs being extracted from the above-mentioned set of 2,010 OGs (ortholog set for supermatrix C, Table 2, Online Resource 1: Fig. S2). Lastly, after extracting OGs with gene multiplications only in bdelloid rotifers and controlling for reduced missing data, we inferred an additional set of 262 SCOGs (ortholog set for supermatrix D, Table 2, Online Resource 1: Fig. S2). Overlap analyses of these ortholog sets showed that they were semi-independent with varying degrees of OG overlap (Online Resource 1: Fig. S3, S4). Specifically, the ortholog sets of supermatrices C and D did not share any OGs with the ortholog set of supermatrix A, whereas the ortholog sets of supermatrices A and B showed the highest OG overlap (168 shared OGs). Lastly, Orthofinder produced an amino-acid supermatrix based on 1,200 OGs that contained single-copy genes for the majority of species (66.7% of species, 8 of the 12 species, supermatrix E before trimming, Table 2). Supermatrix E was the largest in terms of amino-acid alignment sites even after applying the BMGE trimming (206,917 amino-acid alignment sites, see Table 2).

Statistical properties of different species, amino-acid supermatrices and their inferred trees

We observed extreme branch-length heterogeneity within Syndermata as indicated by the LB scores of species in the analyzed supermatrices (e.g., Fig 2e, Online Resource 1: Fig. S6). Overall, species of Bdelloidea and Monogononta showed much lower LB scores in comparison to Acanthocephala and Seisonidea. Specifically, *P. laevis* and *S. nebaliae* were the two species of the ingroup with the highest LB scores when considering all supermatrices under both site-heterogeneous and site-homogeneous models (Fig. 2e, Online Resource 1: Fig. S6). These two species had the highest LB scores, irrespective of whether species of Platyhelminthes were included in the phylogenetic analysis (Fig. 2e, Online Resource 1: Fig. S6).

Amino-acid completeness score was high across supermatrices (ranging from 83.31% to 94.69%) with *P. laevis* being the species with the highest degree of missing data in most datasets (Online Resource 1: Figs. S7–S27, Online Resource 2: Table S2). Screening of the supermatrices and the corresponding inferred trees with AliGROOVE did not show evidence for clades being supported due to strong heterogeneous sequence divergence irrespective of the topology obtained (Online Resource 1: Figs. S28–S43, Online Resource 2: Table S2). Nevertheless, individual sequences of *P. laevis* showed evidence of potential heterogeneous sequence divergence in the similarity-based colored heatmaps and corresponding color-mapped trees produced by AliGROOVE (Online Resource 1: Figs. S28–S43). However, this could also be due to the high proportion of missing data

for *P. laevis* in some of the analyzed supermatrices (e.g., supermatrices A, A50.1, A50.2, E, F, H, Online Resource 1: Figs. S7, S11, S12, S14, S16, S17, S28–S31,S38–S43).

In an attempt reduce possibility for phylogenetic artefacts due to excessive branch-length heterogeneity, we applied a site-removal strategy based on the presence of unique amino acids for some or all species (see methods). Our site-removal strategy resulted in improved levels of branch-length heterogeneity in the analyzed datasets (lower standard deviation of LB scores) but also increased TORCV values (Fig. 2d, Online Resource 2: Table S1). Such conditions of data and tree properties are desirable for avoiding artefacts due to systematic errors. In addition, the above-mentioned site-removal strategy resulted in a reduced proportion of failed symmetry tests of compositional homogeneity in some datasets, showing less potential deviation from model assumptions in these filtered supermatrices (supermatrices: B50.3, C50.3, D50.3, see Online Resource 1: Figs. S44–S64 and Online Resource 2: Table S1). Nevertheless, it is unclear whether this reduced proportion of failed symmetry tests for compositional homogeneity was due to the smaller alignment length of the filtered supermatrices, as the proportion of failed pairwise tests was positively correlated with the size of the dataset (i.e., number of alignment sites, Pearson's r: 0.82, p-value=0.00093, Online Resource 1: Figs. S65–S67).

Topology of Syndermata is dependent on the choice of substitution model in concatenation-based analyses under full taxon sampling

Our model selection procedure always identified empirical profile mixture models as best-fitting for all supermatrices (Online Resource 2: Table S2). More specifically, the LG+C60+F+R5 model was most commonly selected as the best-fit model across supermatrices (Online Resource 2: Table S2). We observed that choice of the substitution model affected the inferred relationships within Gynognathifera (i.e., Micrognathozoa + Syndermata) when Platyhelminthes were included in the analyses (Fig. 2c, Online Resource 1: Figs. 68–129). Overall, Syndermata was recovered as sister to Micrognathozoa with strong support when using a model that accounts for compositional heterogeneity across sites (Fig. 2c, 8 of 9 supermatrices under full taxon sampling, models: LG+C60+F+R5, WAG+C60+F+R5). In contrast, when using a site-homogeneous model for phylogenetic reconstruction, we inferred Micrognathozoa nested within Syndermata in 7 out of 9 cases (Fig. 2c, model: LG+F+R5). In all these cases, Seisonidea was placed as sister to a clade Micrognathozoa + (Acanthocephala + Bdelloidea + Monogononta). Using an empirical profile mixture model, with 21 instead of 61 categories (i.e., LG+C20+F+R5, Online Resource 2: Table S2), also favored the Syndermata hypothesis (7 out of 9 supermatrices, Online Resource 1: Figs.

S109–129). Additionally, all but one Bayesian phylogenetic analyses of supermatrices with full taxon sampling and the CAT+GTR+G4 model also supported the Syndermata with high posterior probability (3 of 4 analyses, Online Resource 1: Figs. S130–S140). In summary, for the majority of cases the Syndermata hypothesis could not be inferred unless a model that accounts for among-site compositional heterogeneity was applied (supermatrices A, A50.1, B, C, D, D50.1). We observed, however, that for two supermatrices the Syndermata hypothesis was inferred under both optimal and suboptimal evolutionary models (site-homogeneous and site-heterogeneous, supermatrices E and B50.1).

Phylogeny of the major subclades of Syndermata inferred from concatenation-based analyses

Maximum-likelihood phylogenetic analyses with the empirical profile mixture models resulted in Seisonidea placed as sister to all other lineages of Syndermata for 7 out of the 9 supermatrices with full taxon sampling (see Online Resource 1: Figs. S68–S87, LG+C60+F+R5, WAG+C60+F+R5). However, the clade Acanthocephala + Bdelloidea + Monogononta (i.e.,, Fig. 1e) did not receive strong branch support in all maximum-likelihood analyses (e.g., supermatrices: A50.1 with 85% UFB support, and B50.1 with 51% UFB support). Selection of the top 50 genes for phylogenetic analysis did not affect this phylogenetic relationship under the same empirical profile mixture models but support of a clade Acanthocephala + Bdelloidea + Monogononta was then greatly reduced (e.g., from 99% UFB support in supermatrix A to 85% UFB support in supermatrix A50.1, Online Resource 1: Figs. S68, S69). Moreover, removal of the distantly related Platyhelminthes from the analyses resulted in Monogononta placed as sister to the rest of Syndermata when analyzing supermatrix F, or as sister to Seisonidea when analyzing supermatrix B50.2 (with low SH-aLRT and UFB support, Online Resource 1: Figs. S74, S85). Furthermore, the branch support in favor of monophyletic Acanthocephala + Bdelloidea + Monogononta (i.e., Seisonidea-sister hypothesis) was reduced when removing Platyhelminthes from supermatrices A50.1, C50.1 and D50.1 (e.g., from 85% in A50.1 to 65% UFB support in A50.2, and from 94% UFB in C50.1 to 63% UFB in C50.2). These observations show: 1) reduced branch support for the Seisonidea-sister hypothesis when selecting a subset of the most reliable genes for analysis as selected based on the criteria used by genesortR, and 2) reduced branch support or lack of support for the Seisonidea-sister hypothesis when excluding amino-acid sequences of the distantly related Platyhelminthes from the phylogenetic analysis.

Since the above-mentioned observations indicated potential attraction of *S. nebaliae* to the distantly related Platyhelminthes, and because our complementary phylogenetic approaches suggested

Monogononta (and not Seisonidea) as sister to all other lineages of Syndermata (see below for the microsynteny-based analyses), we also looked at the effect of removing alignment sites with unique amino acids on the internal phylogenetic relationships of Syndermata (Fig. 2a). For supermatrices B50.3, D50.3, H, I, this alignment-site removal recovered the Pararotatoria hypothesis within Hemirotifera (i.e., the Monogononta-sister hypothesis, Fig. 4). The Pararotatoria, but not Hemirotifera, hypothesis was also supported by analysis of the most stringently filtered dataset (supermatrix G, note: Hemirotifera was nevertheless inferred under the less complex LG+C20+F+R5 model in analysis of supermatrix G). Despite this, removal of alignment sites with unique/private amino acids for *P. laevis* and *S. nebaliae* did not alter the topology in analyses of supermatrix C50.3, that supported Seisonidea as sister to all other Syndermata although with low UFB support (60%, Online Resource 1: Fig. S79). Removing sites with unique amino acids for *P. laevis* and *S. nebaliae* from supermatrix A.50.2 resulted in the recovery of Eurotatoria (Fig. 1c, Online Resource 1: Fig. S71) with low statistical branch support (79% UFB support). This was the only dataset whose analyses resulted in Pararotatoria placed as sister to Eurotatoria when using a site-heterogeneous model (but see also analysis of supermatrix G under LG+F+R5, Online Resource 1: Fig. S94). Overall, we observed that our strategy of removing sites with unique amino acids from the analyzed supermatrices resulted in: 1) an increased proportion of analyses that supported the Hemirotifera and Pararotatoria hypotheses (4/7 and 6/7 of filtered supermatrices respectively for each hypothesis, Fig. 2b), and 2) a reduced proportion of supermatrices that supported the Seisonidea-sister and Lemniscea hypotheses (only 1/7 of filtered supermatrices for each hypothesis respectively, Fig. 2b).

Assessing model adequacy in Bayesian phylogenetic analyses with posterior predictive tests

We performed posterior predictive tests to assess model adequacy with respect to two properties: (a) across-species compositional heterogeneity and (b) mean site-specific amino acid diversity. Our results show that the CAT+GTR+G4 adequately described mean site-specific amino acid diversity in the supermatrices, since the mean predicted values of the statistic did not significantly deviate from the observed site-specific amino-acid diversity in the supermatrices (e.g., *p*-values for supermatrices B50.1, B50.2, B50.3: 0.13, 0.24 and 0.26 respectively, see Online Resource 2: Table S3). In addition, we observed that the $|z|$ score for the same statistic (absolute number of standard deviations of the observed values from mean predicted values) decreased after removing the two species of distantly related Platyhelminthes (see $|z|$ scores for mean site-specific amino-acid diversity in supermatrices A50.1, A50.2, B50.1, B50.2, C50.1, C50.2, D50.1, D50.2). The model

was, therefore, better able to predict mean site-specific diversity of amino acids after removing flatworms from our analyses.

In contrast, the majority of posterior predictive tests for compositional heterogeneity across taxa were rejected, showing that CAT+GTR+G4 does not adequately capture this type of heterogeneity in the supermatrices (but see max. heterogeneity for supermatrices D50.1, D50.2, D50.3). We observed however, that |*z*| scores for mean squared compositional heterogeneity across species decreased for all supermatrices after removing the two species of Platyhelminthes. A similar pattern is observed when using maximum compositional heterogeneity across species as a summary statistic (see Online Resource 2: Table S3). With the exception of supermatrix B50.2, all other supermatrices showed reduced |*z*| scores of maximum compositional heterogeneity after removing *Hymenolepis microstoma* and *Schmidtea mediterranea* from the analyses. Reduced |*z*| scores show that removing these two species results in weaker rejection of the null hypothesis (that the model adequately describes across-species compositional heterogeneity in the supermatrices). It should be noted however, that there is no general pattern concerning how the species-specific |*z*| scores changed across matrix manipulations. Nevertheless, our approach to remove sites with unique amino acids in the two species of Pararotatoria resulted in reduced |*z*| scores concerning the amino-acid compositional deviation of each of these two species. Lastly, *Brachionus calyciflorus*, *H. microstoma* and *L. maerski* consistently showed much higher compositional deviation in comparison to other species in the datasets.

Evaluation of four phylogenetic hypotheses of Syndermata in concatenation-based analyses

We summarized the properties of supermatrices that supported (or not) the four selected phylogenetic hypotheses of Syndermata (see Fig. 3a–d). The Seisonidea-sister hypothesis (Seisonidea as sister to a clade Acanthocephala + Bdelloidea + Monogononta) was inferred by the vast majority of supermatrices under the profile mixture models before removing sites with unique amino acids for *P. laevis* and *S. nebaliae* (10 out of 14 supermatrices). However, we observed that supermatrices whose analyses did not result in the inference of the Seisonidea-sister hypothesis were characterized by lower standard deviation of LB scores (median inferred = 27.65, median not inferred = 26.74), higher TORCV values (median inferred = 0.86, median not inferred = 1.54), and lower saturation scores (median inferred= 0.58, median not inferred = 0.78, Fig. 3a–3d, Online Resource 1: Figs: S141, S142). The same pattern concerning these three properties is observed for the datasets whose analyses supported the Lemniscea hypothesis (Fig. 4b, Online Resource 1: Figs.

S141, S142). In summary, these two hypotheses were therefore inferred under dataset and species-tree conditions that are known to increase possibility of systematic errors (Fig. 3a, 3b).

In contrast, supermatrices and their inferred species trees that supported the Hemirotifera or Pararotatoria hypothesis had on average more desirable properties than supermatrices and corresponding species trees that did not support these two hypotheses (Fig. 3c, 3d). Specifically, datasets that supported the Hemirotifera hypothesis were characterized by lower standard deviation of LB scores (median inferred = 26.54, median not inferred = 27.51), higher TORCV values (median inferred = 1.61, median not inferred = 1.09), and higher saturation scores (median inferred = 0.80, median not inferred = 0.65) than the datasets that did not result in the inference of Hemirotifera (Fig. 3c, Online Resource 1: Figs. S141, S142). In a similar fashion, supermatrices whose analyses resulted in the inference of Pararotatoria were characterized by better values for the above-mentioned dataset- and species-tree properties than supermatrices whose analyses did not support the Pararotatoria hypothesis (Fig. 3d, see also Online Resource 1: Figs. S141–S148). Overall, the Hemirotifera and Pararotatoria hypotheses were therefore supported under dataset and species-tree conditions that are less likely to cause systematic errors.

Species-tree inference of syndermatan relationships from multi-copy orthogroups

All but one species-tree analyses using a combination of single- and multi-copy OGs, and all species present (no. of species = 12), supported the Syndermata hypothesis (topology 3, Fig. 5, datasets A–F). Specifically, the SpeciesRax analysis did not result in a clade of Acanthocephala + Bdelloidea + Monogononta + Seisonidea when we used the default gene trees of Orthofinder for species-tree inference (topology 1, dataset A, Fig. 5). However, when we selected the best-fit models in ModelFinder and recalculated the individual gene trees, we were able to infer syndermatan monophyly irrespective of the species-tree method (Fig. 5, datasets B–F). All species-tree analyses of datasets that included Platyhelminthes (B–F) suggested Seisonidea as sister to all remaining syndermatan lineages (i.e., Acanthocephala, Bdelloidea, Monogononta). This result was stable irrespective of the number of OGs analyzed (see datasets B–F, Fig. 5). We observed, however, that the inferred phylogenetic relationships of Syndermata were dependent on the set species present in the initial OGs. More specifically, we repeated all species-tree analyses after removing all sequences of Platyhelminthes from the individual OGs. The results show that when sequences of Platyhelminthes were not part of the individual MSAs of OGs, then Monogononta emerged as sister to an Acanthocephala + Bdelloidea + Seisonidea clade (the Hemirotifera hypothesis, topology 2, Fig. 5). A clade of Acanthocephala + Seisonidea (the Pararotatoria

776 hypothesis) was not inferred in any of our species-tree analyses that combined information from
777 single- and multi-copy OGs (Fig. 5).
778
779 Microsynteny-based phylogenetic reconstruction of syndermatan relationships
780 The total number of characters (i.e., synteny clusters) used to construct the phylogeny of
781 Syndermata differed slightly depending on the parameters applied for syntenic block detection (*n* =
782 17703, *n* = 17711 and *n* = 17571, see Figs 6a, 6b and Online Resource 1: Fig. S149 respectively).
783 We observed that the majority of synteny clusters were specific to bdelloid rotifers, showing a
784 drastic reduction of synteny conservation across syndermatan genomes (see Figs 6a, 6b). *Schmidtea*
785 *mediterranea* was automatically excluded from the phylogenomic profiles constructed by syntenet,
786 potentially due to the lack of synteny to other genome assemblies in the dataset (see Fig. 6a, 6b,
787 Online Resource 1: Fig. S149). The MK+FQ+ASC+R2 model was selected as best-fit model for all
788 different matrices of binary characters irrespective of the parameters used for synteny block
789 definition. Phylogenetic trees inferred from the binary-data matrices suggested Monogononta as
790 sister to a clade Acanthocephala + Bdelloidea + Seisonidea (i.e., the Hemirotifera hypothesis). The
791 Hemirotifera received strong branch support in all analyses (e.g., Fig. 6C: 99% UFB and 98% SH-
792 aLRT) irrespective of the parameters used for syntenic block detection (Figs. 6c, 6d, Online
793 Resource 1: Fig. S150). Despite this, the phylogenetic relationships among Acanthocephala,
794 Bdelloidea and Monogononta differed across analyses with different synteny-block parameters
795 (Figs 6c, 6d, Online Resource 1: Fig. S150). Only one phylogenetic analysis supported the
796 Pararotatoria hypothesis within Hemirotifera (Fig. 6a, parameters: anchors = 2 and max_gaps = 60),
797 in agreement to the results of our concatenation-based analysis of supermatrix H (Fig. 4), but this
798 relationship was poorly supported in the phylogenetic analyses of microsynteny data (46.1% SH-
799 aLRT and 69% UFB support, Fig. 6a).
800
801 We inferred site-concordance factors (SCF, SCFL) to quantify the strength of the microsynteny
802 signal in favor of the Monogononta-sister and the Seisonidea-sister hypotheses. For five out of six
803 concordance factor analyses, the Monogononta-sister (i.e., Hemirotifera) hypothesis was supported
804 by higher site-concordance factor scores than the Seisonidea-sister hypothesis (i.e., Bdelloidea +
805 Monogononta + Acanthocephala, see Online Resource 1: Fig. S151). Furthermore, maximum-
806 likelihood-based SCFL scores, which are less prone to homoplasy errors than parsimony-based SCF
807 scores (Mo et al., 2023; Kück et al., 2022), showed significantly higher values in support of
808 Hemirotifera than for a clade Bdelloidea + Monogononta + Acanthocephala across all microsynteny
809 parameters (Monogononta-sister or Hemirotifera hypothesis: 44.5%, 99.5% and 97.5%; Seisonidea-

sister or Bdelloidea + Monogononta + Acanthocephala hypothesis: 0.35%, 0.35% and 2.26% respectively; Online Resource 1: Fig. S151).

Discussion

Seeking congruence across analyses concerning the phylogenetic relationships of Syndermata

Our study demonstrates the power of combining several sources of evidence to address challenging phylogenetic questions, such as sequence-based phylogenomics (concatenation- and gene-tree-based) and gene colinearity (here referred to as microsynteny conservation, Simakov et al., 2022). Such integrative approaches have received increased attention in the last decade (Niehuis et al., 2012; Sielaff et al., 2016; Cloutier et al., 2019; Drillon et al., 2020; Ontano et al., 2021; Zhao et al., 2021; Parey et al., 2023). The results of our independent phylogenetic approaches enable us to establish the Hemirotifera hypothesis (i.e., Monogononta-sister hypothesis) as the most plausible scenario of early syndermatan evolution. Specifically, we show that a clade Acanthocephala + Bdelloidea + Seisonidea is inferred by analyses of supermatrices with desirable properties but is also supported by microsynteny-based phylogenetic reconstructions and by species-tree methods that use multi-copy OGs. Furthermore, we show that a clade Acanthocephala + Seisonidea (Pararotatoria) is also supported by analyses of supermatrices with desirable properties and partially also by microsynteny-based phylogenetic analyses. However, species-tree methods that rely on multi- and single-copy orthogroups only supported Hemirotifera when distantly related species of Platyhelminthes had previously been removed from the OGs (Fig. 5). The use of distantly related outgroups is a well-known source of error in phylogenetic reconstructions. This is because distantly related species might be characterized by differences in the evolutionary rates and amino-acid sequence composition, resulting in their artefactual grouping with lineages of the ingroup (Philippe & Laurent, 1998; Li et al., 2012; Pisani et al., 2015; Borowiec et al., 2019). In our analyses, there is a considerable phylogenetic distance between Platyhelminthes and the species of Micrognathozoa + Syndermata (Laumer et al., 2019; Marlétaz et al., 2019), which most likely negatively affected our phylogenetic reconstructions. This is particularly evident in most concatenation-based analyses with the site-homogenous LG+F+R5 model that did not support the Syndermata hypothesis when Platyhelminthes were included in the analyses (Fig. 2c). Our observations of the negative effects of using a distantly related outgroup are in agreement with similar observations in previous phylogenomic analyses of syndermatan relationships (e.g., Mauer et al., 2021).

Moreover, our results illustrate the sensitivity of both gene-tree-based and concatenation-based species-tree methods to outgroup selection, potentially due to long-branch attraction, or more

generally model misspecification (Roch & Warnow, 2015; Roch et al., 2019; see also Vasilikopoulos et al., 2019). Overall, we suggest that the use of a distantly related outgroup without comprehensive sampling of the intermediate outgroup lineages should be avoided, if possible, in future sequence-based phylogenomic studies. On the other hand, genome structural approaches might be less prone to phylogenetic artefacts (see for example Sielaff et al., 2016). Additional whole-genome data from closely related gnathiferan groups (e.g., Micrognathozoa and Gnathostomulida) might facilitate more direct tests of this hypothesis. It is possible that a more comprehensive sampling of outgroup species but only from closely related lineages of Gnathifera, such as Micrognathozoa, Gnathostomulida and Chaetognatha might be beneficial for inferring the internal phylogeny of Syndermata in future sequence-based analyses (see e.g., Wey-Fabrizius et al., 2014). The addition of genomic data from other species of Acanthocephala and Seisonidea might also be beneficial. However, as pointed out by other authors, an increased sampling of closely related outgroup species might not solve the problem completely, as some of these closely related outgroup species might be characterized by compositional and other heterogeneities that could then affect the topology of the ingroup (Borowiec et al., 2019). An acceptable solution would then be to choose a good sampling of only closely related outgroup lineages that also have desirable properties such as reduced heterogeneity of sequence composition and evolutionary rates in relation to the ingroup taxa.

Our evaluation of the properties of supermatrices and their inferred trees that supported the Hemirotifera and Pararotatoria hypotheses provides evidence that the inference of these clades is likely not due to systematic error. On the contrary, supermatrices and corresponding inferred trees that do not support the Hemirotifera and Pararotatoria hypotheses seem to have properties that are associated with increased possibility of systematic error, such as increased levels of branch-length heterogeneity (Struck, 2014; Struck et al., 2014; Kapli et al., 2021). The Pararotatoria hypothesis is also strongly supported by analyses of morphological data providing further evidence to support our preferred hypotheses from concatenation-based analyses (Fig. 4, Ahlrichs, 1997, 1998; Zrzavý, 2001). In contrast to the Hemirotifera hypothesis, however, the microsynteny-based phylogenomic analyses only partially supported the monophyly of Acanthocephala + Seisonidea, as only one of three analyses resulted in the inference of this clade with very low branch support (Fig. 6c). We observed, however, very few informative synteny clusters for inferring the deep phylogeny of Syndermata. Currently, we cannot conclude if this is due to the low quality of the analyzed genomes or more generally due to the low degree of conserved gene colinearity across genomes of Syndermata (Fig. 6). Since most genomes included in our analyses were based on short-read

878 sequencing technologies, and therefore had low degree of contiguity, this question will be answered
879 once highly complete and contiguous genomes from all clades of Syndermata and outgroups
880 become available. The first chromosome-level assembly of a bdelloid rotifer is a promising step in
881 this direction (Simion et al., 2021).
882
883 The Pararotatoria hypothesis was not supported by our species-tree analyses of multi-copy OGs
884 (Fig. 5). Despite this, it is generally accepted that there are many challenges when inferring gene
885 trees at deep evolutionary timescales. Specifically, it is challenging to disentangle biological gene-
886 tree heterogeneity from gene-tree estimation error due to low phylogenetic signal or even
887 systematic error (Roch & Warnow, 2015; Springer & Gatesy, 2016; Bryant & Hahn, 2020; Simion
888 et al., 2020; Vasilikopoulos et al., 2021a). Irrespective of the source of gene-tree errors at deep
889 evolutionary timescales, these errors might affect the accuracy of the corresponding species-tree
890 methods (Roch & Warnow, 2015; Springer & Gatesy, 2016; Roch et al., 2019). Thus, it is possible
891 that our gene-tree-based methods failed to recover Acanthocephala and Seisonidea as sister groups
892 due to gene-tree estimation errors as a result of either low phylogenetic signal or systematic error.
893 The latter hypothesis is supported by the observation that removal of sequences of Platyhelminthes
894 from the MSAs of individual OGs altered the internal topology of Syndermata for these species-tree
895 methods, from a Seisonidea-sister to a Monogononta-sister (i.e., Hemirotifera) hypothesis, similarly
896 to some results from the concatenation-based analyses. Therefore, both the Hemirotifera and
897 Pararotatoria hypotheses remain plausible hypotheses of syndermatan evolution but should be both
898 further corroborated once highly complete and contiguous syndermatan genomes become available.
899
900 Our comprehensive phylogenomic analyses using data- and tree-evaluation approaches identify
901 some phylogenetic hypotheses of syndermatan relationships as less likely than others. For example,
902 the Seisonidea-sister and Lemniscea hypotheses are less well supported by our results as they are
903 not inferred from our microsynteny-based phylogenetic reconstructions. Additionally, statistical
904 branch support for a clade of Acanthocephala + Bdelloidea + Monogononta is reduced when
905 selecting the most reliable genes for concatenated analysis, and disappears in the absence of a
906 distantly related outgroup in some sequence-based analyses (concatenation- or gene-tree-based).
907 Moreover, further evaluation of the properties of the supermatrices and inferred trees that supported
908 these two hypotheses (Seisonidea-sister and Lemniscea) suggested that they are inferred under
909 dataset and species-tree properties typically associated with systematic errors (Figs. 3a and 3b).
910 Hence, these latter two hypotheses are not widely supported from analyses of different types of
911 data, tree reconstruction and data-evaluation methods. Although we cannot rule out these two

hypotheses completely, especially given that they were inferred by the majority of sequence-based analyses, we consider them as less likely based on our results. Furthermore, our observation that the Lemniscea and Seisonidea-sister hypotheses were inferred under conditions with elevated possibility of systematic error, despite being the most frequently inferred hypotheses in sequence-based analyses, suggests that the consensus to species phylogenies should ideally rely on methodologically diverse approaches and different types of data, including morphology and genome structures, rather than exclusively on sequence-based analyses. It should be noted, however, that except for Pararotatoria, none of the other three hypotheses that we evaluated receives strong support from morphology so far, a phenomenon that is relatively common in molecular systematics (Pisani et al., 2007). This underlines the importance of critical assessment of the results of both molecular and morphological studies for resolving these conflicts through the process of reciprocal illumination (e.g., Ragsdale & Baldwin, 2010; Gustafson et al., 2021; Sharma et al., 2021).

Implications for the evolution of morphological characters, reproductive modes and parasitic lifestyles within Syndermata

A clade of Acanthocephala + Seisonidea (Pararotatoria) as sister to Bdelloidea is consistent with prevalent views concerning the evolution of endoparasitism within Syndermata (Herlyn, 2021). Specifically, it is currently hypothesized that the endoparasitic lifestyle of Acanthocephala evolved via an intermediate epibiotic (i.e., epizoic) stage on jawed arthropods, such as the one observed in species of the genus *Seison* (Seisonidea). This hypothesis states that there has been a transition from a free-living lifestyle in the common ancestor of Syndermata to an epizoic (or even ectoparasitic, Ricci et al., 1993) lifestyle in the stem lineage of Pararotatoria and a subsequent transition to an endoparasitic lifestyle in the stem lineage of Acanthocephala (and also the addition of a definite gnathostome host in Acanthocephala, Herlyn et al., 2003; Wey-Fabrizius et al., 2014; Sielaff et al., 2016; Herlyn, 2021).

Another important result of our study is that the Eurotatoria hypothesis (i.e., that Bdelloidea and Monogononta are sister groups) seems unlikely, as it was recovered in the analyses of only two supermatrices, but only one of these was using a site-heterogeneous model. This result is congruent with most molecular studies to date (e.g., Garey et al., 1996, 1998; Witek et al., 2008). Similarly to previous hypotheses for the evolution of endoparasitism in Acanthocephala via an intermediate epizoic stage (Herlyn et al., 2003; Herlyn, 2021), one could hypothesize a transition from sexual reproduction to obligate asexuality through an intermediate stage of facultative sexual reproduction within Syndermata, as has been suggested in other organisms (Larose et al., 2023). If Bdelloidea

and Monogononta were indeed sister groups, a plausible explanation for the evolution of reproductive modes within Syndermata would be that there was a transition from sexual reproduction in the common ancestor of Syndermata to facultative sexual reproduction in the stem lineage of Eurotatoria and subsequent complete loss of sex in Bdelloidea. This could also be supported by the conditional presence of non-canonical meiosis in Bdelloidea and Monogononta that would then represent the ancestral state of Eurotatoria (Terwagne et al., 2022). However, our results show that such a hypothesis is unlikely, as do most molecular studies to date (e.g., Witek et al., 2008; Wey-Fabrizius et al., 2014; Sielaff et al., 2016; Mauer et al., 2021). Consequently, an evolutionarily independent modification of the meiotic machinery in Bdelloidea and in Monogononta resulting in obligate or facultative asexuality is more likely following the phylogenomic results presented here. However, it should be emphasized that the hypothesis of an independent evolution of a non-canonical meiosis in Bdelloidea and Monogononta depends on whether this modified meiosis is indeed present in all species of Bdelloidea and Monogononta. Until now, there has been only one detailed cytological study of oogenesis in one bdelloid species (*Adineta vaga*) and a reinterpretation of old cytological results from one monogonont species (Terwagne et al., 2022). Further cytological studies of more species of Monogononta and Bdelloidea could provide additional tests of these hypotheses. Sexual reproduction with separate sexes is probably the ancestral state of Syndermata, since there is no evidence that sexual reproduction can be regained once it is lost. Sexual reproduction with separate sexes in the common ancestor of Syndermata is supported by the presence of males and females in all syndermatan groups except Bdelloidea, but the evolutionary sequence of events among different reproductive modes within Syndermata remains a mystery.

Finally, our hypothesis on the evolution of reproductive modes within Syndermata also depends on the reproductive mode on their closest outgroup; the Micrognathozoa. However, evidence for the reproductive mode of *L. maerski* is not conclusive. To date, only evidence of females can be considered reliable, suggesting that Micrognathozoa reproduce parthenogenetically (Kristensen & Funch, 2000). Despite this, there is also evidence of sculptured eggs besides smooth-shelled eggs, so sexual reproduction could also occur (De Smet, 2002). Moreover, young stages of *L. maerski* reportedly exhibit paired refractive bodies which could represent testicles, suggesting that *L. maerski* might be a protandrous hermaphrodite (Sørensen & Kristensen, 2015). Therefore, although males have not been observed so far, the above-described features suggest that the presence of males, either as separate or protandrous individuals, cannot be excluded. More studies on the

reproductive mode of Micrognathozoa will facilitate formulating more detailed hypotheses on the evolution of reproductive modes within Syndermata.

The Hemirotifera and Pararotatoria hypotheses also necessitate a reevaluation of the evolution of several morphological and ecological characters within Syndermata. For example, characters such as the ciliated corona of Bdelloidea and Monogononta may represent the ancestral state of Syndermata with secondary modification in the stem lineage of Pararotatoria. On the one hand, locomotory ciliation is present in other groups of Gnathifera, such as Micrognathozoa and Gnathostomulida, but the cilia cover larger regions of the body in these groups than in Bdelloidea and Monogononta (Sterrer, 1972; Kristensen & Funch, 2000; Bekkouche & Worsaae, 2016; Sørensen et al., 2016). On the other hand, most species of Bdelloidea and Monogononta have a well-developed ciliated corona in the anterior part of their body, whereas Seisonidea have a reduced corona with minimal ciliation and Acanthocephala lack ciliation altogether (Ricci et al., 1993; Mark Welch, 2000). Therefore, there is likely a trend for reduction of locomotory ciliation within Pararotatoria, from the ciliated corona in the common syndermatan ancestor to the partial and complete loss of ciliation in Seisonidea and Acanthocephala respectively. These features are probably secondary modifications connected to the epizoic or endoparasitic lifestyle of Seisonidea and Acanthocephala. The need for reinterpretation of morphological evolution might apply to additional characters that are considered synapomorphies of Rotifera *sensu stricto* such as the presence of a muscular pharynx (i.e., mastax) that is specialized and unique in Seisonidea (Ricci et al., 1993; Segers & Melone, 1998), while according to current knowledge is absent in Acanthocephala (Mark Welch, 2000). Moreover, species belonging to the sister group of Syndermata, the Micrognathozoa, possess a muscular pharynx with hard pieces that are very similar to rotifer trophi, and are even more complex than those of rotifers (Kristensen & Funch, 2000; De Smet, 2002; Sørensen, 2003).Thus, it is not unlikely that the typical mastax as it is known from Monogononta and Bdelloidea was present in the common ancestor of Syndermata with subsequent secondary modifications in species of Pararotatoria, as a result of their epizoic or endoparasitic lifestyle.

References

Ababneh, F., L. S. Jermiin, C. Ma, & J. Robinson, 2006. Matched-pairs tests of homogeneity with applications to homologous nucleotide sequences. Bioinformatics 22: 1225–1231. https://doi.org/10.1093/bioinformatics/btl064.

1012 Ahlrichs, W. H., 1995. Ultrastruktur und Phylogenie von *Seison nebaliae* (Grube 1859) und *Seison*
1013 *annulatus* (Claus 1876). Hypothesen zu phylogenetischen Verwandschaftsverhältnissen innerhalb
1014 der Bilateria. Cuvilier, Göttingen.

1015 Ahlrichs, W. H., 1997. Epidermal ultrastructure of *Seison nebaliae* and *Seison annulatus*, and a
1016 comparison of epidermal structures within the Gnathifera. Zoomorphology 117: 41–48.
1017 https://doi.org/10.1007/s004350050028.

1018 Ahlrichs, W. H., 1998. Spermatogenesis and ultrastructure of the spermatozoa of *Seison nebaliae*
1019 (Syndermata). Zoomorphology 118: 255–261. https://doi.org/10.1007/s004350050074.

1020 Almeida-Silva, F., T. Zhao, K. K. Ullrich, M. E. Schranz, & Y. Van de Peer, 2023. Syntenet: an
1021 R/Bioconductor package for the inference and analysis of synteny networks. Bioinformatics 39:
1022 btac806. https://doi.org/10.1093/bioinformatics/btac806.

1023 Bekkouche, N., & L. Gąsiorowski, 2022. Careful amendment of morphological data sets improves
1024 phylogenetic frameworks: re-evaluating placement of the fossil *Amiskwia sagittiformis*. Journal of
1025 Systematic Palaeontology 20: 2109217. https://doi.org/10.1080/14772019.2022.2109217.

1026 Bekkouche, N., & K. Worsaae, 2016. Nervous system and ciliary structures of Micrognathozoa
1027 (Gnathifera): evolutionary insight from an early branch in Spiralia. Royal Society Open Science 3:
1028 160289. https://doi.org/10.1098/rsos.160289.

1029 Bollback, J. P., 2002. Bayesian model adequacy and choice in phylogenetics. Molecular Biology
1030 and Evolution 19: 1171–1180, https://doi.org/10.1093/oxfordjournals.molbev.a004175.

1031 Borowiec, M. L., C. Rabeling, S. G. Brady, B. L. Fisher, T. R. Schultz, & P. S. Ward, 2019.
1032 Compositional heterogeneity and outgroup choice influence the internal phylogeny of the ants.
1033 Molecular Phylogenetics and Evolution 134: 111–121.
1034 https://doi.org/10.1016/j.ympev.2019.01.024.

1035 Bowker, A. H., 1948. A test for symmetry in contingency tables. Journal of the American Statistical
1036 Association 43: 572–574. https://doi.org/10.2307/2280710.

1037 Bradley, R. K., A. Roberts, M. Smoot, S. Juvekar, J. Do, C. Dewey, I. Holmes, & L. Pachter, 2009.
1038 Fast statistical alignment. PLoS Computational Biology 5: e1000392.
1039 https://doi.org/10.1371/journal.pcbi.1000392.

1040 Bryant, D., & M. W. Hahn, 2020. The concatenation question In Scornavacca, C., F. Delsuc, & N.
1041 Galtier (eds), Phylogenetics in the genomic era. No commercial publisher | Authors' open access
1042 book: 3.4:1–3.4:23. https://hal.science/hal-02535651.

1043 Buchfink, B., K. Reuter, & H.-G. Drost, 2021. Sensitive protein alignments at tree-of-life scale
1044 using DIAMOND. Nature Methods 18: 366–368. https://doi.org/10.1038/s41592-021-01101-x.

1045 Clément, P., 1993. The phylogeny of rotifers: molecular, ultrastructural and behavioural data.
1046 Hydrobiologia 255: 527–544. https://doi.org/10.1007/BF00025882.

1047 Cloutier, A., T. B. Sackton, P. Grayson, M. Clamp, A. J. Baker, & S. V. Edwards, 2019. Whole-
1048 genome analyses resolve the phylogeny of flightless birds (Palaeognathae) in the presence of an
1049 empirical anomaly zone. Systematic Biology 68: 937–955. https://doi.org/10.1093/sysbio/syz019.

1050 Criscuolo, A., & S. Gribaldo, 2010. BMGE (Block Mapping and Gathering with Entropy): a new
1051 software for selection of phylogenetic informative regions from multiple sequence alignments.
1052 BMC Evolutionary Biology 10: 210. https://doi.org/10.1186/1471-2148-10-210.

1053 De Smet, W. H., 2002. A new record of *Limnognathia maerski* Kristensen & Funch, 2000
1054 (Micrognathozoa) from the subantarctic Crozet Islands, with redescription of the trophi. Journal of
1055 Zoology 258: 381–393. https://doi.org/10.1017/S095283690200153X.

1056 Di Franco, A., R. Poujol, D. Baurain, & H. Philippe, 2019. Evaluating the usefulness of alignment
1057 filtering methods to reduce the impact of errors on evolutionary inferences. BMC Evolutionary
1058 Biology 19: 21. https://doi.org/10.1186/s12862-019-1350-2.

1059 Drillon, G., R. Champeimont, F. Oteri, G. Fischer, & A. Carbone, 2020. Phylogenetic reconstruction
1060 based on synteny block and gene adjacencies. Molecular Biology and Evolution 37: 2747–2762,
1061 https://doi.org/10.1093/molbev/msaa114.

1062 Emms, D. M., & S. Kelly, 2018. STAG: species tree inference from all genes. BioRxiv 267914.
1063 https://doi.org/10.1101/267914.

1064 Emms, D. M., & S. Kelly, 2019. OrthoFinder: phylogenetic orthology inference for comparative
1065 genomics. Genome Biology 20: 238. https://doi.org/10.1186/s13059-019-1832-y.

1066 Ferraguti, M., & G. Melone, 1999. Spermiogenesis in *Seison nebaliae* (Rotifera, Seisonidea):
1067 further evidence of a rotifer-acanthocephalan relationship. Tissue and Cell 31: 428–440.
1068 https://doi.org/10.1054/tice.1999.0012.

1069 Feuda, R., M. Dohrmann, W. Pett, H. Philippe, O. Rota-Stabelli, N. Lartillot, G. Wörheide, & D.
1070 Pisani, 2017. Improved modeling of compositional heterogeneity supports sponges as sister to all
1071 other animals. Current Biology 27: 3864–3870. https://doi.org/10.1016/j.cub.2017.11.008

1072 Fontaneto, D., 2014. Molecular phylogenies as a tool to understand diversity in rotifers.
1073 International Review of Hydrobiology 99: 178–187. https://doi.org/10.1002/iroh.201301719.

1074 Fontaneto, D., & W. H. De Smet, 2015. Rotifera In Schmidt-Rhaesa, A. (ed), Handbook of zoology,
1075 volume 3 Gastrotricha and Gnathifera. De Gruyter, Berlin: 217–300.

1076 Fontaneto, D., & U. Jondelius, 2011. Broad taxonomic sampling of mitochondrial cytochrome c
1077 oxidase subunit I does not solve the relationships between Rotifera and Acanthocephala.
1078 Zoologischer Anzeiger 250: 80–85. http://dx.doi.org/10.1016/j.jcz.2010.11.005.

1079 Funch, P., M. V. Sørensen, & M. Obst, 2005. On the phylogenetic position of Rotifera - have we
1080 come any further?. Hydrobiologia 546: 11–28. https://doi.org/10.1007/s10750-005-4093-6.

1081 Fussmann, G. F., 2011. Rotifers: excellent subjects for the study of macro- and microevolutionary
1082 change. Hydrobiologia 662: 11–18. https://doi.org/10.1007/s10750-010-0515-1.

García-Varela, M., & S. A. Nadler, 2006. Phylogenetic relationships among Syndermata inferred from nuclear and mitochondrial gene sequences. Molecular Phylogenetics and Evolution 40: 61–72. https://doi.org/10.1016/j.ympev.2006.02.010.

Garey, J. R., T. J. Near, M. R. Nonnemacher, & S. A. Nadler, 1996. Molecular evidence for Acanthocephala as a subtaxon of Rotifera. Journal of Molecular Evolution 43: 287–292. https://doi.org/10.1007/BF02338837.

Garey, J. R., A. Schmidt-Rhaesa, T. J. Near, & S. A. Nadler, 1998. The evolutionary relationships of rotifers and acanthocephalans. Hydrobiologia 387: 83–91. https://doi.org/10.1023/A:1017060902909.

Grabherr, M. G., B. J. Haas, M. Yassour, J. Z. Levin, D. A. Thompson, I. Amit, X. Adiconis, L. Fan, R. Raychowdhury, Q. Zeng, Z. Chen, E. Mauceli, N. Hacohen, A. Gnirke, N. Rhind, F. Di Palma, B. W. Birren, C. Nusbaum, K. Lindblad-Toh, N. Friedman, & A. Regev, 2011. Full-length transcriptome assembly from RNA-Seq data without a reference genome. Nature Biotechnology 29: 644–652. https://doi.org/10.1038/nbt.1883.

Guindon, S., J. F. Dufayard, V. Lefort, M. Anisimova, W. Hordijk, & O. Gascuel, 2010. New algorithms and methods to estimate maximum-likelihood phylogenies: assessing the performance of PhyML 3.0. Systematic Biology 59: 307–321. https://doi.org/10.1093/sysbio/syq010.

Gustafson, G. T., K. B. Miller, M. C. Michat, Y. Alarie, S. M. Baca, M. Balke, & A. E. Z. Short, 2021. The enduring value of reciprocal illumination in the era of insect phylogenomics: a response to Cai et al. (2020). Systematic Entomology 46: 473–486. https://doi.org/10.1111/syen.12471.

Hankeln, T., A. R. Wey-Fabrizius, H. Herlyn, M. Weber, M. P. Nesnidal, T. H. Struck, & A. Witek, 2014. Phylogeny of platyzoan taxa based on molecular data In Wägele, J. W., & T. Bartolomaeus (eds), Deep metazoan phylogeny: the backbone of the tree of life. De Gruyter: 105–126.

Herlyn, H., 2021. Thorny-headed worms (Acanthocephala): jaw-less members of jaw-bearing worms that parasitize jawed arthropods and jawed vertebrates In K. De Baets, & J. W. Huntley (eds), The evolution and fossil record of parasitism, Topics in Geobiology, vol 49. Springer, Cham: 273–313. https://doi.org/10.1007/978-3-030-42484-8_8.

Herlyn, H., O. Piskurek, J. Schmitz, U. Ehlers, & H. Zischler, 2003. The syndermatan phylogeny and the evolution of acanthocephalan endoparasitism as inferred from 18S rDNA sequences. Molecular Phylogenetics and Evolution 26: 155–164. https://doi.org/10.1016/S1055-7903(02)00309-3.

Hoang, D. T., O. Chernomor, A. von Haeseler, B. Q. Minh, & S. V. Le, 2018. UFBoot2: improving the ultrafast bootstrap approximation. Molecular Biology and Evolution 35: 518–522. https://doi.org/10.1093/molbev/msx281.

Howe, K. L., B. J. Bolt, M. Shafie, P. Kersey, & M. Berriman, 2017. WormBase ParaSite − a comprehensive resource for helminth genomics. Molecular and Biochemical Parasitology 215: 2–10. https://doi.org/10.1016/j.molbiopara.2016.11.005.

1120 Huerta-Cepas, J., F. Serra, & P. Bork, 2016. ETE 3: reconstruction, analysis, and visualization of
1121 phylogenomic data. Molecular Biology and Evolution 33: 1635–1638.
1122 https://doi.org/10.1093/molbev/msw046.

1123 Hunter, J. D., 2007. Matplotlib: a 2D graphics environment. Computing in Science & Engineering
1124 9: 90–95. https://doi.org/10.1109/MCSE.2007.55.

1125 Hur, J. H., K. Van Doninck, M. L. Mandigo, & M. Meselson, 2009. Degenerate tetraploidy was
1126 established before bdelloid rotifer families diverged. Molecular Biology and Evolution 26: 375–
1127 383. https://doi.org/10.1093/molbev/msn260.

1128 Jermiin, L. S., V. Jayaswal, F. Ababneh, & J. Robinson, 2008. Phylogenetic model evaluation In
1129 Keith, J. M. (ed), Bioinformatics. Methods in molecular biology™, vol 452. Humana Press,
1130 Totowa: 331–363. https://doi.org/10.1007/978-1-60327-159-2_16.

1131 Jermiin, L. S., D. R. Lovell, B. Misof, P. G. Foster, & J. Robinson, 2020. Detecting and visualising
1132 the impact of heterogeneous evolutionary processes on phylogenetic estimates. BioRxiv 828996.
1133 https://doi.org/10.1101/828996.

1134 Jiao, X., T. Flouri, B. Rannala, & Z. Yang, 2020. The impact of cross-species gene flow on species
1135 tree estimation. Systematic Biology 69: 830–847. https://doi.org/10.1093/sysbio/syaa001.

1136 Kalyaanamoorthy, S., B. Q. Minh, T. K. F. Wong, A. von Haeseler, & L. S. Jermiin, 2017.
1137 ModelFinder: fast model selection for accurate phylogenetic estimates. Nature Methods 14: 587–
1138 589. http://dx.doi.org/10.1038/nmeth.4285.

1139 Kapli, P., T. Flouri, & M. J. Telford, 2021. Systematic errors in phylogenetic trees. Current Biology
1140 31: R59–R64. http://dx.doi.org/10.1016/j.cub.2020.11.043.

1141 Kapli, P., Z. Yang, & M. J. Telford, 2020. Phylogenetic tree building in the genomic age. Nature
1142 Reviews Genetics 21: 428–444. http://dx.doi.org/10.1038/s41576-020-0233-0.

1143 Kim, D. H., M. S. Kim, A. Hagiwara, & J. S. Lee, 2021. The genome of the minute marine rotifer
1144 *Proales similis*: genome-wide identification of 401 G protein-coupled receptor (GPCR) genes.
1145 Comparative Biochemistry and Physiology - Part D: Genomics and Proteomics 39: 100861.
1146 https://doi.org/10.1016/j.cbd.2021.100861.

1147 Klopfstein, S., T. Massingham, & N. Goldman, 2017. More on the best evolutionary rate for
1148 phylogenetic analysis. Systematic Biology 66: 769–785. https://doi.org/10.1093/sysbio/syx051.

1149 Kozlov, A. M., D. Darriba, T. Flouri, B. Morel, & A. Stamatakis, 2019. RAxML-NG: a fast,
1150 scalable and user-friendly tool for maximum likelihood phylogenetic inference. Bioinformatics 35:
1151 4453–4455. https://doi.org/10.1093/bioinformatics/btz305.

1152 Kristensen, R. M., & P. Funch, 2000. Micrognathozoa: a new class with complicated jaws like those
1153 of Rotifera and Gnathostomulida. Journal of Morphology 246: 1–49. https://doi.org/10.1002/1097-
1154 4687(200010)246:1%3C1::AID-JMOR1%3E3.0.CO;2-D.

1155 Kubatko, L. S., & J. H. Degnan, 2007. Inconsistency of phylogenetic estimates from concatenated
1156 data under coalescence. Systematic Biology 56: 17–24.
1157 https://doi.org/10.1080/10635150601146041.

1158 Kück, P., S. A. Meid, C. Groß, J. W. Wägele, & B. Misof, 2014. AliGROOVE--visualization of
1159 heterogeneous sequence divergence within multiple sequence alignments and detection of inflated
1160 branch support. BMC Bioinformatics 15: 294. https://doi.org/10.1186/1471-2105-15-294.

1161 Kück, P., J. Romahn, & K. Meusemann, 2022. Pitfalls of the site-concordance factor (sCF) as
1162 measure of phylogenetic branch support. NAR Genomics and Bioinformatics 4: lqac064.
1163 https://doi.org/10.1093/nargab/lqac064

1164 Lanyon, S. M., 1988. The stochastic mode of molecular evolution: what consequences for
1165 systematic investigations?. The Auk 105: 565–573. https://doi.org/10.1093/auk/105.3.565.

1166 Larose, C., G. Lavanchy, S. Freitas, D. J. Parker, & T. Schwander, 2023. Facultative
1167 parthenogenesis: a transient state in transitions between sex and obligate asexuality in stick insects?.
1168 Peer Community Journal 3: e60. https://doi.org/10.24072/pcjournal.283

1169 Lartillot, N., 2020. PhyloBayes: Bayesian phylogenetics using site-heterogeneous models. In
1170 Scornavacca, C., F. Delsuc, & N. Galtier (eds), Phylogenetics in the genomic era. No commercial
1171 publisher | Authors open access book: 1.5:1–1.5:16. https://hal.science/hal-02535342.

1172 Lartillot, N., H. Brinkmann, & H. Philippe, 2007. Suppression of long-branch attraction artefacts in
1173 the animal phylogeny using a site-heterogeneous model. BMC Evolutionary Biology 7: S4.
1174 https://doi.org/10.1186/1471-2148-7-S1-S4.

1175 Lartillot, N., & H. Philippe, 2004. A Bayesian mixture model for across-site heterogeneities in the
1176 amino-acid replacement process. Molecular Biology and Evolution 21: 1095–1109.
1177 https://doi.org/10.1093/molbev/msh112.

1178 Lartillot, N., N. Rodrigue, D. Stubbs, & J. Richer, 2013. PhyloBayes MPI: phylogenetic
1179 reconstruction with infinite mixtures of profiles in a parallel environment. Systematic Biology 62:
1180 611–615. https://doi.org/10.1093/sysbio/syt022.

1181 Lasek-Nesselquist, E., 2012. A mitogenomic re-evaluation of the bdelloid phylogeny and
1182 relationships among the Syndermata. PLoS ONE 7: e43554.
1183 https://doi.org/10.1371/journal.pone.0043554.

1184 Laumer, C. E., N. Bekkouche, A. Kerbl, F. Goetz, R. C. Neves, M. V Sørensen, R. M. Kristensen,
1185 A. Hejnol, C. W. Dunn, G. Giribet, & K. Worsaae, 2015. Spiralian phylogeny informs the evolution
1186 of microscopic lineages. Current Biology 25: 2000–2006.
1187 http://dx.doi.org/10.1016/j.cub.2015.06.068.

1188 Laumer, C. E., R. Fernández, S. Lemer, D. Combosch, K. M. Kocot, A. Riesgo, S. C. S. Andrade,
1189 W. Sterrer, M. V. Sørensen, & G. Giribet, 2019. Revisiting metazoan phylogeny with genomic
1190 sampling of all phyla. Proceedings of the Royal Society B: Biological Sciences 286: 20190831.
1191 https://doi.org/10.1098/rspb.2019.0831.

Le, S. Q., O. Gascuel, & N. Lartillot, 2008. Empirical profile mixture models for phylogenetic reconstruction. Bioinformatics 24: 2317–2323. https://doi.org/10.1093/bioinformatics/btn445.

Lehmann, J., P. F. Stadler, & V. Krauss, 2013. Near intron pairs and the metazoan tree. Molecular Phylogenetics and Evolution 66: 811–823. http://dx.doi.org/10.1016/j.ympev.2012.11.012.

Letunic, I., & P. Bork, 2021. Interactive tree of life (iTOL) v5: an online tool for phylogenetic tree display and annotation. Nucleic Acids Research 49: W293–W296. https://doi.org/10.1093/nar/gkab301.

Li, C., K. A. Matthes-Rosana, M. Garcia, & G. J. P. Naylor, 2012. Phylogenetics of Chondrichthyes and the problem of rooting phylogenies with distant outgroups. Molecular Phylogenetics and Evolution 63: 365–373. https://doi.org/10.1016/j.ympev.2012.01.013.

Lorenzen, S., 1985. Phylogenetic aspects of pseudocoelomate evolution In Morris, S. C., J. D. George, R. Gibson, & H. M. Platt (eds), The origins and relationships of lower invertebrates. Clarendon Press, Oxford.

Maddison, W. P., 1997. Gene trees in species trees. Systematic Biology 46: 523–536. https://doi.org/10.1093/sysbio/46.3.523.

Mark Welch, D. B., 2000. Evidence from a protein-coding gene that acanthocephalans are rotifers. Invertebrate Biology 119: 17–26. https://doi.org/10.1111/j.1744-7410.2000.tb00170.x.

Mark Welch, D. B., 2005. Bayesian and maximum likelihood analyses of rotifer-acanthocephalan relationships. Hydrobiologia 546: 47–54. https://doi.org/10.1007/s10750-005-4100-y.

Mark Welch, D. B., J. L. Mark Welch, & M. Meselson, 2008. Evidence for degenerate tetraploidy in bdelloid rotifers. Proceedings of the National Academy of Sciences of the United States of America 105: 5145–5149. https://doi.org/10.1073/pnas.0800972105.

Marlétaz, F., K. T. C. A. Peijnenburg, T. Goto, N. Satoh, & D. S. Rokhsar, 2019. A new spiralian phylogeny places the enigmatic arrow worms among gnathiferans. Current Biology 29: 312–318. https://doi.org/10.1016/j.cub.2018.11.042.

Mauer, K., S. L. Hellmann, M. Groth, A. C. Fröbius, H. Zischler, T. Hankeln, & H. Herlyn, 2020. The genome, transcriptome, and proteome of the fish parasite *Pomphorhynchus laevis* (Acanthocephala). PLoS ONE 15: e0232973. https://doi.org/10.1371/journal.pone.0232973.

Mauer, K. M., H. Schmidt, M. Dittrich, A. C. Fröbius, S. L. Hellmann, H. Zischler, T. Hankeln, & H. Herlyn, 2021. Genomics and transcriptomics of epizoic Seisonidea (Rotifera, syn. Syndermata) reveal strain formation and gradual gene loss with growing ties to the host. BMC Genomics 22: 604. https://doi.org/10.1186/s12864-021-07857-y.

McCarthy, C. G. P., P. O. Mulhair, K. Siu-Ting, C. J. Creevey, & M. J. O'Connell, 2023. Improving orthologous signal and model fit in datasets addressing the root of the animal phylogeny. Molecular Biology and Evolution 40: msac276. https://doi.org/10.1093/molbev/msac276.

McKinney, W., 2010. Data structures for statistical computing in python. In van der Walt, S., & J. Millman (eds), Proceedings of the 9th Python in Science Conference: 51–56. https://doi.org/10.25080/Majora-92bf1922-00a.

Melone, G., C. Ricci, H. Segers, & R. L. Wallace, 1998. Phylogenetic relationships of phylum Rotifera with emphasis on the families of Bdelloidea. Hydrobiologia 387: 101–107. https://doi.org/10.1023/A:1017057619574.

Mendes, F. K., & M. W. Hahn, 2018. Why concatenation fails near the anomaly zone. Systematic Biology 67: 158–169. https://doi.org/10.1093/sysbio/syx063.

Min, G.-S., & J.-K. Park, 2009. Eurotatorian paraphyly: revisiting phylogenetic relationships based on the complete mitochondrial genome sequence of *Rotaria rotatoria* (Bdelloidea: Rotifera: Syndermata). BMC Genomics 10: 533. https://doi.org/10.1186/1471-2164-10-533.

Minh, B. Q., M. W. Hahn, & R. Lanfear, 2020a. New methods to calculate concordance factors for phylogenomic datasets. Molecular Biology and Evolution 37: 2727–2733, https://doi.org/10.1093/molbev/msaa106.

Minh, B. Q., H. A. Schmidt, O. Chernomor, D. Schrempf, M. D. Woodhams, A. von Haeseler, & R. Lanfear, 2020b. IQ-TREE 2: New models and efficient methods for phylogenetic inference in the genomic era. Molecular Biology and Evolution 37: 1530–1534. https://doi.org/10.1093/molbev/msaa015.

Misof, B., B. Meyer, B. M. von Reumont, P. Kück, K. Misof, & K. Meusemann, 2013. Selecting informative subsets of sparse supermatrices increases the chance to find correct trees. BMC Bioinformatics 14: 348. https://doi.org/10.1186/1471-2105-14-348.

Mo, Y. K., R. Lanfear, M. W. Hahn, & B. Q. Minh, 2023. Updated site concordance factors minimize effects of homoplasy and taxon sampling. Bioinformatics 39: btac741. https://doi.org/10.1093/bioinformatics/btac741.

Mongiardino Koch, N., 2021. Phylogenomic subsampling and the search for phylogenetically reliable loci. Molecular Biology and Evolution 38: 4025–4038. https://doi.org/10.1093/molbev/msab151.

Morel, B., A. M. Kozlov, A. Stamatakis, & G. J. Szöllősi, 2020. GeneRax: a tool for species-tree-aware maximum likelihood-based gene family tree inference under gene duplication, transfer, and loss. Molecular Biology and Evolution 37: 2763–2774. https://doi.org/10.1093/molbev/msaa141.

Morel, B., P. Schade, S. Lutteropp, T. A. Williams, G. J. Szöllősi, & A. Stamatakis, 2022. SpeciesRax: a tool for maximum likelihood species tree inference from gene family trees under duplication, transfer, and loss. Molecular Biology and Evolution 39: msab365. https://doi.org/10.1093/molbev/msab365.

Naser-Khdour, S., B. Q. Minh, W. Zhang, E. A. Stone, R. Lanfear, & D. Bryant, 2019. The prevalence and impact of model violations in phylogenetic analysis. Genome Biology and Evolution 11: 3341–3352. https://doi.org/10.1093/gbe/evz193.

Near, T. J., 2002. Acanthocephalan phylogeny and the evolution of parasitism. Integrative and Comparative Biology 42: 668–677. https://doi.org/10.1093/icb/42.3.668.

Nguyen, L.-T., H. A. Schmidt, A. Von Haeseler, & B. Q. Minh, 2015. IQ-TREE: a fast and effective stochastic algorithm for estimating maximum-likelihood phylogenies. Molecular Biology and Evolution 32: 268–274. https://doi.org/10.1093/molbev/msu300.

Niehuis, O., G. Hartig, S. Grath, H. Pohl, J. Lehmann, H. Tafer, A. Donath, V. Krauss, C. Eisenhardt, J. Hertel, M. Petersen, C. Mayer, K. Meusemann, R. S. Peters, P. F. Stadler, R. G. Beutel, E. Bornberg-Bauer, D. D. McKenna, & B. Misof, 2012. Genomic and morphological evidence converge to resolve the enigma of Strepsiptera. Current Biology 22: 1309–1313. https://doi.org/10.1016/j.cub.2012.05.018.

Nowell, R. W., P. Almeida, C. G. Wilson, T. P. Smith, D. Fontaneto, A. Crisp, G. Micklem, A. Tunnacliffe, C. Boschetti, & T. G. Barraclough, 2018. Comparative genomics of bdelloid rotifers: insights from desiccating and nondesiccating species. PLoS Biology 16: e2004830. https://doi.org/10.1371/journal.pbio.2004830.

Nowell, R. W., C. G. Wilson, P. Almeida, P. H. Schiffer, D. Fontaneto, L. Becks, F. Rodriguez, I. R. Arkhipova, & T. G. Barraclough, 2021. Evolutionary dynamics of transposable elements in bdelloid rotifers. eLife 10: e63194. https://doi.org/10.7554/eLife.63194.

Ontano, A. Z., G. Gainett, S. Aharon, J. A. Ballesteros, L. R. Benavides, K. F. Corbett, E. Gavish-Regev, M. S. Harvey, S. Monsma, C. E. Santibáñez-López, E. V. W. Setton, J. T. Zehms, J. A. Zeh, D. W. Zeh, & P. P. Sharma, 2021. Taxonomic sampling and rare genomic changes overcome long-branch attraction in the phylogenetic placement of Pseudoscorpions. Molecular Biology and Evolution 38: 2446–2467. https://doi.org/10.1093/molbev/msab038.

Parey, E., A. Louis, J. Montfort, O. Bouchez, C. Roques, C. Iampietro, J. Lluch, A. Castinel, C. Donnadieu, T. Desvignes, C. F. Bucao, E. Jouanno, M. Wen, S. Mejri, R. P. Dirks, H. J. Jansen, C. V Henkel, W.-J. Chen, M. Zahm, C. Cabau, C. Klopp, A. W. Thompson, M. Robinson-Rechavi, I. Braasch, G. Lecointre, J. Bobe, J. H. Postlethwait, C. Berthelot, H. Roest Crollius, & Y. Guiguen, 2023. Genome structures resolve the early diversification of teleost fishes. Science 379: 572–575. https://doi.org/10.1126/science.abq4257.

Philippe, H., H. Brinkmann, D. V. Lavrov, D. T. J. Littlewood, M. Manuel, G. Wörheide, & D. Baurain, 2011. Resolving difficult phylogenetic questions: why more sequences are not enough. PLoS Biology 9: e1000602. https://doi.org/10.1371/journal.pbio.1000602.

Philippe, H., R. Derelle, P. Lopez, K. Pick, C. Borchiellini, N. Boury-Esnault, J. Vacelet, E. Renard, E. Houliston, E. Quéinnec, C. Da Silva, P. Wincker, H. Le Guyader, S. Leys, D. J. Jackson, F. Schreiber, D. Erpenbeck, B. Morgenstern, G. Wörheide, & M. Manuel, 2009. Phylogenomics revives traditional views on deep animal relationships. Current Biology 19: 706–712. https://doi.org/10.1016/j.cub.2009.02.052.

Philippe, H., & J. Laurent, 1998. How good are deep phylogenetic trees?. Current Opinion in Genetics & Development 8: 616–623. https://doi.org/10.1016/S0959-437X(98)80028-2.

Philippe, H., & B. Roure, 2011. Difficult phylogenetic questions: more data, maybe; better methods, certainly. BMC Biology 9: 91. https://doi.org/10.1186/1741-7007-9-91.

Phillips, M. J., & D. Penny, 2003. The root of the mammalian tree inferred from whole mitochondrial genomes. Molecular Phylogenetics and Evolution 28: 171–185. https://doi.org/10.1016/S1055-7903(03)00057-5.

Pisani, D., M. J. Benton, & M. Wilkinson, 2007. Congruence of morphological and molecular phylogenies. Acta Biotheoretica 55: 269–281. https://doi.org/10.1007/s10441-007-9015-8.

Pisani, D., W. Pett, M. Dohrmann, R. Feuda, O. Rota-Stabelli, H. Philippe, N. Lartillot, & G. Wörheide, 2015. Genomic data do not support comb jellies as the sister group to all other animals. Proceedings of the National Academy of Sciences 112: 15402–15407. https://doi.org/10.1073/pnas.1518127112.

R Core Team, 2021. R: a language and environment for statistical computing. Vienna, Austria, https://www.r-project.org/.

Ragsdale, E. J., & J. G. Baldwin, 2010. Resolving phylogenetic incongruence to articulate homology and phenotypic evolution: a case study from Nematoda. Proceedings of the Royal Society B: Biological Sciences Royal Society 277: 1299–1307. https://doi.org/10.1098/rspb.2009.2195.

Ricci, C., 1998. Are lemnisci and proboscis present in the Bdelloidea?. Hydrobiologia 387–388: 93–96. https://doi.org/10.1023/A:1017091104243.

Ricci, C., G. Melone, & C. Sotgia, 1993. Old and new data on Seisonidea (Rotifera). Hydrobiologia 255: 495–511. https://doi.org/10.1007/BF00025879.

Roch, S., M. Nute, & T. Warnow, 2019. Long-branch attraction in species tree estimation: inconsistency of partitioned likelihood and topology-based summary methods. Systematic Biology 68: 281–297. https://doi.org/10.1093/sysbio/syy061.

Roch, S., & T. Warnow, 2015. On the robustness to gene tree estimation error (or lack thereof) of coalescent-based species tree methods. Systematic Biology 64: 663–676. https://doi.org/10.1093/sysbio/syv016.

Rozanski, A., H. Moon, H. Brandl, J. M. Martín-Durán, M. A. Grohme, K. Hüttner, K. Bartscherer, I. Henry, & J. C. Rink, 2019. PlanMine 3.0—improvements to a mineable resource of flatworm biology and biodiversity. Nucleic Acids Research 47: D812–D820. https://doi.org/10.1093/nar/gky1070.

Salichos, L., & A. Rokas, 2013. Inferring ancient divergences requires genes with strong phylogenetic signals. Nature 497: 327–331. http://dx.doi.org/10.1038/nature12130.

Schultz, D. T., S. H. D. Haddock, J. V. Bredeson, R. E. Green, O. Simakov, & D. S. Rokhsar, 2023. Ancient gene linkages support ctenophores as sister to other animals. Nature 618: 110–117. https://doi.org/10.1038/s41586-023-05936-6.

Segers, H., & G. Melone, 1998. A comparative study of trophi morphology in Seisonidea (Rotifera). Journal of Zoology 244: 201–207. https://doi.org/10.1111/j.1469-7998.1998.tb00025.x.

Sharma, P. P., J. A. Ballesteros, & C. E. Santibáñez-López, 2021. What is an "arachnid"? Consensus, consilience, and confirmation bias in the phylogenetics of Chelicerata. Diversity 13: 568. https://doi.org/10.3390/d13110568.

Sielaff, M., H. Schmidt, T. H. Struck, D. Rosenkranz, D. B. Mark Welch, T. Hankeln, & H. Herlyn, 2016. Phylogeny of Syndermata (syn. Rotifera): mitochondrial gene order verifies epizoic Seisonidea as sister to endoparasitic Acanthocephala within monophyletic Hemirotifera. Molecular Phylogenetics and Evolution 96: 79–92. https://doi.org/10.1016/j.ympev.2015.11.017.

Simakov, O., J. Bredeson, K. Berkoff, F. Marletaz, T. Mitros, D. T. Schultz, B. L. O'Connell, P. Dear, D. E. Martinez, R. E. Steele, R. E. Green, C. N. David, & D. S. Rokhsar, 2022. Deeply conserved synteny and the evolution of metazoan chromosomes. Science Advances 8: eabi5884. https://doi.org/10.1126/sciadv.abi5884.

Simion, P., F. Delsuc, & H. Philippe, 2020. To what extent current limits of phylogenomics can be overcome? In Scornavacca, C., F. Delsuc, & N. Galtier (eds), Phylogenetics in the genomic era. No commercial publisher | Authors' open access book: 2.1:1–2.1:34. https://hal.archives-ouvertes.fr/hal-02535366.

Simion, P., J. Narayan, A. Houtain, A. Derzelle, L. Baudry, E. Nicolas, R. Arora, M. Cariou, C. Cruaud, F. R. Gaudray, C. Gilbert, N. Guiglielmoni, B. Hespeels, D. K. L. Kozlowski, K. Labadie, A. Limasset, M. Llirós, M. Marbouty, M. Terwagne, J. Virgo, R. Cordaux, E. G. J. Danchin, B. Hallet, R. Koszul, T. Lenormand, J. F. Flot, & K. Van Doninck, 2021. Chromosome-level genome assembly reveals homologous chromosomes and recombination in asexual rotifer *Adineta vaga*. Science Advances 7: eabg4216. https://doi.org/10.1126/sciadv.abg4216.

Siu-Ting, K., M. Torres-Sánchez, D. San Mauro, D. Wilcockson, M. Wilkinson, D. Pisani, M. J. O'Connell, & C. J. Creevey, 2019. Inadvertent paralog inclusion drives artifactual topologies and timetree estimates in phylogenomics. Molecular Biology and Evolution 36: 1344–1356. https://doi.org/10.1093/molbev/msz067.

Smith, M. L., & M. W. Hahn, 2021. New approaches for inferring phylogenies in the presence of paralogs. Trends in Genetics 37: 174–187. https://doi.org/10.1016/j.tig.2020.08.012.

Sørensen, M. V., R. M. Kristensen, & K. Worsaae, 2016. The Gnathifera. Phyla Gnathostomulida, Rotifera (including Acanthocephala), and Micrognathozoa In Brusca, R. C., W. Moore, & S. M. Shuster (eds), Invertebrates. Sinauer Associates: 613–634.

Sørensen, M. V., & R. M. Kristensen, 2015. Micrognathozoa In Schmidt-Rhaesa, A. (ed), Handbook of zoology, Volume 3 Gastrotricha and Gnathifera. De Gruyter, Berlin: 197–216.

Sørensen, M. V., 2002. On the evolution and morphology of the rotiferan trophi, with a cladistic analysis of Rotifera. Journal of Zoological Systematics and Evolutionary Research 40: 129–154. https://doi.org/10.1046/j.1439-0469.2002.00188.x.

Sørensen, M. V., 2003. Further structures in the jaw apparatus of *Limnognathia maerski* (Micrognathozoa), with notes on the phylogeny of the Gnathifera. Journal of Morphology 255: 131–145. https://doi.org/10.1002/jmor.10038.

Sørensen, M. V., P. Funch, E. Willerslev, A. J. Hansen, & J. Olesen, 2000. On the phylogeny of the Metazoa in the light of Cycliophora and Micrognathozoa. Zoologischer Anzeiger 239: 297–318.

Sørensen, M. V., & G. Giribet, 2006. A modern approach to rotiferan phylogeny: combining morphological and molecular data. Molecular Phylogenetics and Evolution 40: 585–608. https://doi.org/10.1016/j.ympev.2006.04.001.

Springer, M. S., & J. Gatesy, 2016. The gene tree delusion. Molecular Phylogenetics and Evolution 94: 1–33. http://dx.doi.org/10.1016/j.ympev.2015.07.018.

Stamatakis, A., & A. M. Kozlov, 2020. Efficient maximum likelihood tree building methods. In Scornavacca, C., F. Delsuc, & N. Galtier (eds), Phylogenetics in the genomic era. No commercial publisher | Authors open access book: 1.2 :1–1.2:18, https://hal.science/hal-02535285v2.

Steenwyk, J. L., T. J. Buida III, A. L. Labella, Y. Li, X.-X. Shen, & A. Rokas, 2021. PhyKIT: a broadly applicable UNIX shell toolkit for processing and analyzing phylogenomic data. Bioinformatics 37: 2325–2331. https://doi.org/10.1093/bioinformatics/btab096.

Steenwyk, J. L., D. C. Goltz, T. J. Buida III, Y. Li, X.-X. Shen, & A. Rokas, 2022. OrthoSNAP: a tree splitting and pruning algorithm for retrieving single-copy orthologs from gene family trees. PLOS Biology 20: e3001827. https://doi.org/10.1371/journal.pbio.3001827.

Sterrer, W., 1972. Systematics and evolution within the Gnathostomulida. Systematic Zoology 21: 151–173. https://doi.org/10.2307/2412286.

Storch, V., & U. Welsch, 1969. Über den Aufbau des Rotatorienintegumentes. Zeitschrift für Zellforschung und Mikroskopische Anatomie 95: 405–414. https://doi.org/10.1007/BF00995213.

Struck, T. H., 2014. TreSpEx-Detection of misleading signal in phylogenetic reconstructions based on tree information. Evolutionary Bioinformatics 10: 51–67. https://doi.org/10.4137/EBO.S14239.

Struck, T. H., A. R. Wey-Fabrizius, A. Golombek, L. Hering, A. Weigert, C. Bleidorn, S. Klebow, N. Iakovenko, B. Hausdorf, M. Petersen, P. Kück, H. Herlyn, & T. Hankeln, 2014. Platyzoan paraphyly based on phylogenomic data supports a noncoelomate ancestry of Spiralia. Molecular Biology and Evolution 31: 1833–1849. http://dx.doi.org/10.1093/molbev/msu143.

Terwagne, M., E. Nicolas, B. Hespeels, L. Herter, J. Virgo, C. Demazy, A. C. Heuskin, B. Hallet, & K. Van Doninck, 2022. DNA repair during nonreductional meiosis in the asexual rotifer *Adineta vaga*. Science advances 8: eadc8829. https://doi.org/10.1126/sciadv.adc8829.

Tihelka, E., C. Cai, M. Giacomelli, J. Lozano-Fernandez, O. Rota-Stabelli, D. Huang, M. S. Engel, P. C. J. Donoghue, & D. Pisani, 2021. The evolution of insect biodiversity. Current Biology 31: R1299–R1311. https://doi.org/10.1016/j.cub.2021.08.057.

Vasilikopoulos, A., M. Balke, R. G. Beutel, A. Donath, L. Podsiadlowski, J. M. Pflug, R. M. Waterhouse, K. Meusemann, R. S. Peters, H. E. Escalona, C. Mayer, S. Liu, L. Hendrich, Y. Alarie, D. T. Bilton, F. Jia, X. Zhou, D. R. Maddison, O. Niehuis, & B. Misof, 2019. Phylogenomics of the superfamily Dytiscoidea (Coleoptera: Adephaga) with an evaluation of phylogenetic conflict and systematic error. Molecular Phylogenetics and Evolution 135: 270–285. https://doi.org/10.1016/j.ympev.2019.02.022.

Vasilikopoulos, A., M. Balke, S. Kukowka, J. M. Pflug, S. Martin, K. Meusemann, L. Hendrich, C. Mayer, D. R. Maddison, O. Niehuis, R. G. Beutel, & B. Misof, 2021a. Phylogenomic analyses clarify the pattern of evolution of Adephaga (Coleoptera) and highlight phylogenetic artefacts due to model misspecification and excessive data trimming. Systematic Entomology 46: 991–1018. https://doi.org/10.1111/syen.12508.

Vasilikopoulos, A., G. T. Gustafson, M. Balke, O. Niehuis, R. G. Beutel, & B. Misof, 2021b. Resolving the phylogenetic position of Hygrobiidae (Coleoptera: Adephaga) requires objective statistical tests and exhaustive phylogenetic methodology: a response to Cai et al. (2020). Molecular Phylogenetics and Evolution 162: 106923. https://doi.org/10.1016/j.ympev.2020.106923.

Von Haffner, K., 1950. Organisation und systematische Stellung der Acanthocephalen. Zoologischer Anzeiger 145: 243–274.

Wallace, R. L., 2002. Rotifers: exquisite metazoans. Integrative and Comparative Biology 42: 660–667. https://doi.org/10.1093/icb/42.3.660.

Wallace, R. L., & R. A. Colburn, 1989. Phylogenetic relationships within phylum Rotifera: orders and genus *Notholca* In Ricci, C., T. W. Snell, & C. E. King (eds), Rotifer Symposium V. Developments in Hydrobiology, vol 52. Springer, Dordrecht: 311–318. https://doi.org/10.1007/978-94-009-0465-1_37.

Wallace, R. L., C. Ricci, & G. Melone, 1996. A cladistic analysis of pseudocoelomate (aschelminth) morphology. Invertebrate Biology 115: 104–112. https://doi.org/10.2307/3227041.

Wang, Y., H. Tang, J. D. Debarry, X. Tan, J. Li, X. Wang, T. H. Lee, H. Jin, B. Marler, H. Guo, J. C. Kissinger, & A. H. Paterson, 2012. MCScanX: a toolkit for detection and evolutionary analysis of gene synteny and collinearity. Nucleic Acids Research 40: e49. https://doi.org/10.1093/nar/gkr1293.

Waskom, M. L., 2021. Seaborn: statistical data visualization. Journal of Open Source Software 6: 3021. https://doi.org/10.21105/joss.03021.

Wey-Fabrizius, A. R., H. Herlyn, B. Rieger, D. Rosenkranz, A. Witek, D. B. Mark Welch, I. Ebersberger, & T. Hankeln, 2014. Transcriptome data reveal syndermatan relationships and suggest the evolution of endoparasitism in Acanthocephala via an epizoic stage. PLoS ONE 9: e88618. https://doi.org/10.1371/journal.pone.0088618.

Whelan, S., I. Irisarri, & F. Burki, 2018. PREQUAL: detecting non-homologous characters in sets of unaligned homologous sequences. Bioinformatics 34: 3929–3930. https://dx.doi.org/10.1093/bioinformatics/bty448.

Winnepenninckx, B., T. Backeljau, L. Y. Mackey, J. M. Brooks, R. De Wachter, S. Kumar, & J. R. Garey, 1995. 18S rRNA data indicate that Aschelminthes are polyphyletic in origin and consist of at least three distinct clades. Molecular Biology and Evolution 12: 1132–1137. https://doi.org/10.1093/oxfordjournals.molbev.a040287.

Winnepenninckx, B. M. H., T. Backeljau, & R. M. Kristensen, 1998. Relations of the new phylum Cycliophora. Nature 393: 636–638. https://doi.org/10.1038/31377.

Witek, A., H. Herlyn, I. Ebersberger, D. B. Mark Welch, & T. Hankeln, 2009. Support for the monophyletic origin of Gnathifera from phylogenomics. Molecular Phylogenetics and Evolution 53: 1037–1041. http://dx.doi.org/10.1016/j.ympev.2009.07.031.

Witek, A., H. Herlyn, A. Meyer, L. Boell, G. Bucher, & T. Hankeln, 2008. EST based phylogenomics of Syndermata questions monophyly of Eurotatoria. BMC Evolutionary Biology 8: 345. https://doi.org/10.1186/1471-2148-8-345.

Zhang, C., & S. Mirarab, 2022. ASTRAL-Pro 2: ultrafast species tree reconstruction from multi-copy gene family trees. Bioinformatics 38: 4949–4950. https://doi.org/10.1093/bioinformatics/btac620.

Zhang, C., C. Scornavacca, E. K. Molloy, & S. Mirarab, 2020. ASTRAL-Pro: quartet-based species-tree inference despite paralogy. Molecular Biology and Evolution 37: 3292–3307. https://doi.org/10.1093/molbev/msaa139.

Zhao, T., A. Zwaenepoel, J.-Y. Xue, S.-M. Kao, Z. Li, M. E. Schranz, & Y. Van de Peer, 2021. Whole-genome microsynteny-based phylogeny of angiosperms. Nature Communications 12: 3498. https://doi.org/10.1038/s41467-021-23665-0.

Zrzavý, J., 2001. The interrelationships of metazoan parasites: a review of phylum- and higher-level hypotheses from recent morphological and molecular phylogenetic analyses. Folia Parasitologica 48: 81–103. https://doi.org/10.14411/fp.2001.013.

Figure captions

Fig. 1 Competing hypotheses concerning the phylogenetic relationships of Syndermata based on the results of previous molecular and morphological studies. **a)** Seisonidea is the sister group of Acanthocephala (Pararotatoria hypothesis); **b)** Acanthocephala is the sister group of Bdelloidea (Lemniscea hypothesis); **c)** Bdelloidea and Monogononta are sister groups (Eurotatoria hypothesis); **d)** Seisonidea is the sister group of a clade Acanthocephala + Bdelloidea + Monogononta (i.e., Seisonidea-sister hypothesis); **e)** Monogononta is the sister group of a clade Acanthocephala + Bdelloidea + Seisonidea (Hemirotifera or Monogononta-sister hypothesis); **f)** Acanthocephala is the sister group of a clade Bdelloidea + Monogononta + Seisonidea (i.e., Rotifera *sensu stricto*)

Fig. 2 a) Workflow describing the steps for generating the different supermatrices analyzed in the present study (see also Table 2); **b)** Summary of phylogenetic results from concatenation-based analyses before and after removing alignment sites with unique amino acids for some or all species (see methods and Table 2). Input datasets are supermatrices before removing sites with private amino-acids (third column in Fig. 2a, five supermatrices: A50.2, B50.2, C50.2, D50.2, F) whereas output datasets are supermatrices after these alignment sites have been removed (fourth column in Fig. 2a, seven supermatrices: A50.3, B50.3, C50.3, D50.3, G, H, I). Support (i.e., inference) or not of the different hypotheses is denoted as 1 and 0 respectively; **c)** Number of inferred trees supporting or not (1 and 0 respectively) the Syndermata hypothesis depending on the evolutionary model (only supermatrices with full taxon sampling). Results are based on the maximum-likelihood analyses using the empirical profile mixture model with 61classes (site-heterogeneous) and the LG+F+R5 model (site-homogeneous); **d)** Effect of removing alignment sites with unique amino acids on the properties of inferred trees and supermatrices (input supermatrices are before removing these sites whereas output supermatrices are after removing these sites, see third and fourth column in Fig. 2a). Overall, this site-removal approach results in increased TORCV values and reduced branch-length heterogeneity (LB score standard deviation); **e)** Extreme branch-length heterogeneity among subgroups of Syndermata. Distribution of LB scores for each species across the different supermatrices (only supermatrices with reduced taxon sampling and before removing sites with unique amino acids are taken into account, see third column in Fig. 2a)

Fig. 3 Evaluation of the species-tree and supermatrix properties that supported or not (1 or 0 respectively) the four selected phylogenetic hypotheses within Syndermata. Left: supermatrices (dots) are plotted in the 2D space based on 1) the branch-length heterogeneity of their inferred trees (standard deviation of LB scores) and 2) TORCV scores. Right: barplots show median values of LB score standard deviation and median TORCV values separately for the supermatrices whose analyses resulted in the inference or not (1, 0) of each hypothesis. **a)** Seisonidea-sister hypothesis (i.e., monophyly of Acanthocephala + Bdelloidea + Monogononta); **b)** Lemniscea hypothesis; **c)** Hemirotifera hypothesis; **d)** Pararotatoria hypothesis

Fig. 4 Phylogenetic tree with the best log-likelihood score that resulted from the maximum-likelihood phylogenetic analysis of supermatrix H using the LG+C60+F+R5 model. The tree was rooted with *Limnognathia maerski*. Statistical branch support is shown on the tree nodes based on 2000 SH-aLRT and 1000 ultrafast bootstrap and replicates. This phylogenetic tree displays features

associated with more reliable combinations of data and methods across concatenation-based analyses

Fig. 5 Results of gene-tree-based phylogenetic analyses of Syndermata depending on the dataset and species-tree method used. Rows in the grid correspond to different subsets of orthogroups and their inferred gene trees and colors show the different topologies obtained depending on the species-tree method applied (different columns represent different species-tree inference methods). Dataset A consists of all the gene trees that were inferred automatically by Orthofinder (*n* = 2,010). Datasets A–F correspond to orthogroup multiple sequence alignments and their inferred trees by including sequences of Platyhelminthes. Datasets G–K correspond to sets of orthogroups and gene trees that were inferred after the two species of Platyhelminthes were removed from the multiple sequence alignments of individual orthogroups

Fig. 6 Results of microsynteny-based phylogenomic profiling and phylogenetic reconstructions of Syndermata. **a)** phylogenomic profiling of synteny clusters across syndermatan genomes when using the parameters: anchors = 2 and max_gaps = 60 for syntenic block definition; **b)** phylogenomic profiling of syntenic clusters across syndermatan genomes when using the parameters: anchors = 3 and max_gaps = 60 for synteny-block definition. Columns in the heatmaps correspond to different synteny clusters that are present or absent in different species. Each synteny cluster (i.e., character) corresponds to a set of anchored genes within a syntenic block across species. Colors show the number of genes per cluster for each species (0, 1, 2 or ≥ 3). Multiple genes for a species in a cluster could be due to uncollapsed haplotypes or polyploidization. Initials in the rows of the heatmaps correspond to the species names (av: *Adineta vaga*, ar: *Adineta ricciae*, rr: *Rotaria sordida*, rc: *Rotaria socialis*, dc: *Didymodactylos carnosus*, bc: *Brachionus calyciflorus*, ps: *Proales similis*, pl: *Pomphorhynchus laevis*, sn: *Seison nebaliae*, hm: *Hymenolepis microstoma*); **c)** Cladogram showing the inferred phylogenetic relationships of Syndermata when using the parameters anchors = 2 and max_gaps = 60 for syntenic block definition; **d)** Cladogram showing the inferred phylogenetic relationships of Syndermata when using the parameters anchors = 3 and max_gaps = 60 for syntenic block definition. Since some internal branches were very short, only the topology of the inferred species trees is depicted. Statistical branch support of the inferred trees is shown based on 2000 SH-aLRT and 1000 ultrafast bootstrap replicates

1549

1550

1551

1552

1553

1554

Table 1 Genome and transcriptome datasets analyzed in the present study and their associated statistics. BUSCO gene completeness was assessed using the Metazoa lineage (i.e., 954 genes in total). Percentage of gene completeness is based only on complete BUSCO genes in each proteome (fragmented genes are not taken into account, see also Online Resource 1: Fig. S1). For the transcriptome of *Limnognathia maerski*, raw reads were downloaded from the NCBI-SRA database (accession: SRR2131287) and processed as described in the text to produce a set of protein sequences

Species	**Taxonomic group**	**Dataset type**	**Genome assembly accession (Genbank-NCBI)**	**No. of protein-coding genes***	**BUSCO completeness of predicted proteomes (%)**	**Source of gene annotation**	**Date of retrieval**
Hymenolepis microstoma (Dujardin, 1845)	Platyhelminthes	Genome	GCA_000469805.3	10,139	74.00	WormBase Parasite v. 17.0 (annotation: v. 2018-10-WormBase)	04.07.2022
Schmidtea mediterranea Benazzi, Baguna, Ballester & del Papa, 1975	Platyhelminthes	Genome	GCA_002600895.1	22,045	77.70	PlanMine v. 3.0 (annotation: v. 2 high conf.)	28.09.2022
Limnognathia maerski Kristensen & Funch, 2000	Micrognathozoa	Transcriptome	Not applicable	16,811	70.90	Not applicable	07.07.2022
Seison nebaliae Grube, 1861	Syndermata, Seisonidea	Genome	GCA_023231475.1	11,502	65.00	Genbank-NCBI	28.09.2022
Pomphorhynchus laevis (Zoega in Müller, 1776)	Syndermata, Acanthocephala	Genome	GCA_012934845.2	12,073	54.10	Genbank-NCBI	28.09.2022
Proales similis de Beauchamp, 1907	Syndermata, Monogononta	Genome	GCA_019059635.1	9,469	76.80	Annotated in the present study	03.10.2022
Brachionus calyciflorus Pallas, 1766	Syndermata, Monogononta	Genome	GCA_002922825.1	23,548	90.40	Genbank-NCBI	28.09.2022
Didymodactylos carnosus Milne, 1916	Syndermata, Bdelloidea	Genome	GCA_905250885.1	46,863	82.80	Genbank-NCBI	28.09.2022
Rotaria socialis (Kellicott, 1888)	Syndermata, Bdelloidea	Genome	GCA_905331475.1	32,760	88.90	Genbank-NCBI	28.09.2022
Rotaria sordida (Western, 1893)	Syndermata, Bdelloidea	Genome	GCA_905251635.1	39,313	89.50	Genbank-NCBI	28.09.2022
Adineta vaga (Davis, 1873)	Syndermata, Bdelloidea	Genome	GCA_021613535.1	31,335	88.50	Genbank-NCBI	28.09.2022

Adineta ricciae Segers & Shiel, 2005	Syndermata, Bdelloidea	Genome	GCA_905250025.1	46,588	88.70	Genbank-NCBI	28.09.2022

*Note: number of protein-coding genes is given after removing pseudogenes, alternative gene transcripts or isoforms

Table 2 Overview, statistics and description of amino-acid supermatrices analyzed in the present study. Note that the number of genes refers to the original supermatrices before trimming hypervariable sites (i.e., for supermatrix E) or removing columns with private/unique amino acids (see also Fig. 1). More detailed statistics are given in the Online Resource 2: Table S1. PI: parsimony-informative sites, OG: orthogroup, SCOG: single-copy orthogroup

Supermatrix ID	No. of species	No. of genes	No. of alignment sites	No. of PI sites	Description
supermatrix A	12	345	86,409	43,019	Selected SCOGs with minimum of 10 species present
supermatrix B	12	233	56,310	28,560	Selected decisive SCOGs (i.e., with >= 1 species from each taxonomic group). Added decisive genes with species-specific gene multiplications only in one non-bdelloid species (max. five copies; we kept the copy with the highest average pairwise non-ambiguous coverage in the alignments)
supermatrix C	12	267	86,214	37,560	Extracted SCOGs from decisive multi-copy OGs using orthoSNAP (requirements: max. five copies per species in each multi-copy OG and min. 10 species in each extracted SCOG).
Supermatrix D	12	262	79,411	38,043	Extracted decisive multi-copy OGs for which only bdelloids have multiple copies. Used OrthoSNAP to extract SCOGs within bdelloid clade and merged the sequences of one of these SCOGs with the single copies of non-bdelloid species in the same OG.
Supermatrix E	12	1,200	206,917	120,319	Original supermatrix used by Orthofinder after trimming it with BMGE (all OGs for which at least 66.6% of species are single-copy)
Supermatrix F	10	1,200	206,917	95,141	Removed the two species of Platyhelminthes from supermatrix E
Supermatrix G	10	1,200	65,508	23,768	Removed all alignment sites with unique amino acids for any species from supermatrix F
Supermatrix H	10	1,200	162,015	45,201	Removed sites with unique amino acids for *S. nebaliae* and/or *P. laevis* from supermatrix F (only if there were no unique amino-acids for additional species on the same column)
Supermatrix I	10	1,200	146,698	64,394	Removed sites that contained unique amino acids for any of the species from supermatrix F
supermatrix A50.1	12	50	17,007	6,558	Keep only the best 50 genes from supermatrix A using genesortR
supermatrix A50.2	10	50	17,007	5,057	Removed the two species of Platyhelminthes from supermatrix A50.1
supermatrix A50.3	10	50	14,303	4,195	Removed sites with unique amino acids for *S. nebaliae* and/or *P. laevis* from supermatrix A50.2
supermatrix B50.1	12	50	17,184	7,265	Keep only the best 50 genes from supermatrix B using genesortR
supermatrix B50.2	10	50	17,184	5,741	Removed the two species of Platyhelminthes from supermatrix B50.1
supermatrix B50.3	10	50	13,839	4,578	Removed sites with unique amino acids for *S. nebaliae* and/or *P. laevis* from supermatrix B50.2
supermatrix C50.1	12	50	22,100	7,280	Keep only the best 50 genes from supermatrix C using genesortR
supermatrix C50.2	10	50	22,100	5,658	Removed the two species of Platyhelminthes from supermatrix C50.1
supermatrix C50.3	10	50	19,990	5,051	Removed sites with unique amino acids for *S. nebaliae* and/or *P. laevis* from supermatrix C50.2
supermatrix D50.1	12	50	16,271	5,959	Keep only the best 50 genes from supermatrix D using genesortR
supermatrix D50.2	10	50	16,271	4,629	Removed the two species of Platyhelminthes from supermatrix D50.1
supermatrix D50.3	10	50	12,884	3,524	Removed sites with unique amino acids for *S. nebaliae* and/or *P. laevis* from supermatrix D50.2

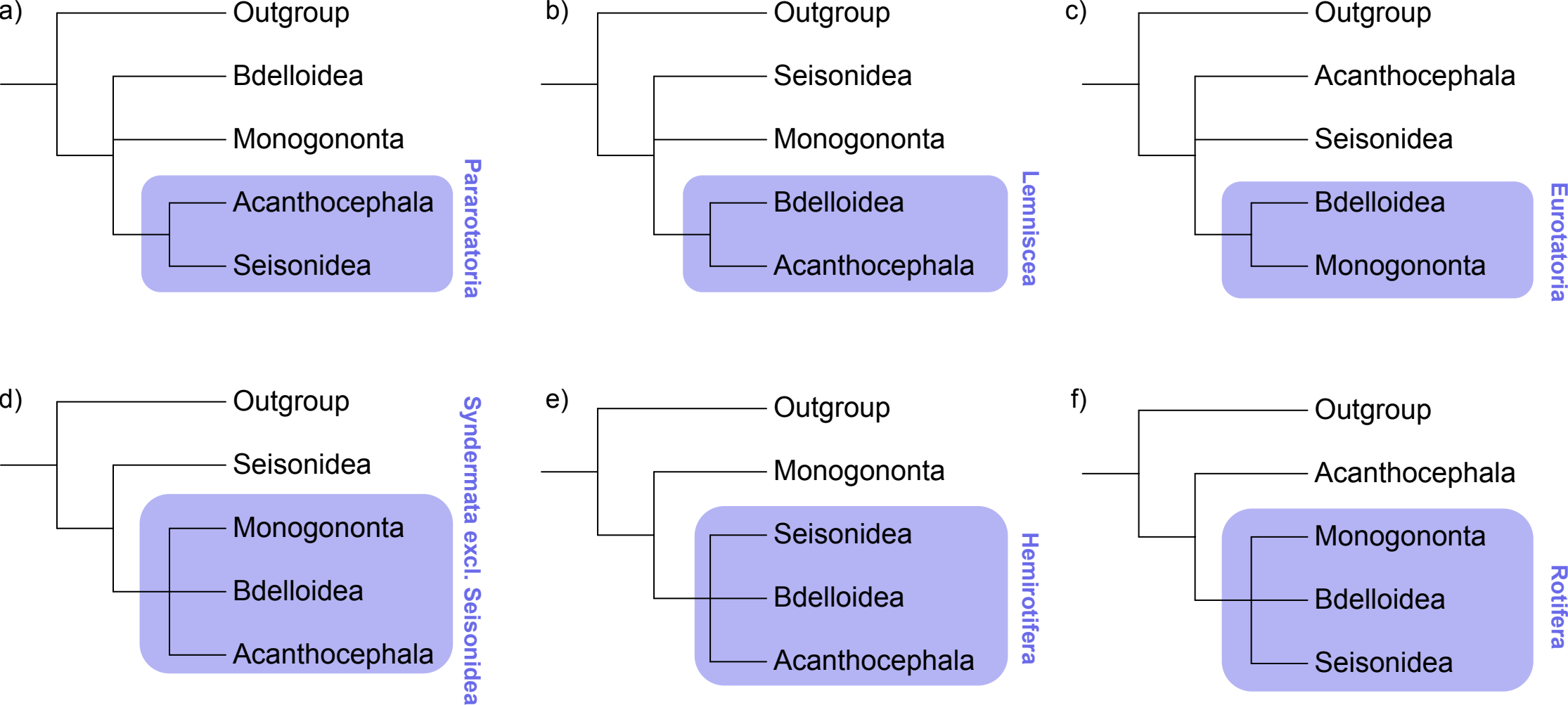
a)
Outgroup
Bdelloidea
Monogononta
Acanthocephala
Seisonidea
Pararotatoria
b)
Outgroup
Seisonidea
Monogononta
Bdelloidea
Acanthocephala
Lemniscea
c)
Outgroup
Acanthocephala
Seisonidea
Bdelloidea
Monogononta
Eurotatoria
d)
Outgroup
Seisonidea
Monogononta
Bdelloidea
Acanthocephala
Syndermata excl. Seisonidea
e)
Outgroup
Monogononta
Seisonidea
Bdelloidea
Acanthocephala
Hemirotifera
f)
Outgroup
Acanthocephala
Monogononta
Bdelloidea
Seisonidea
Rotifera

a)

Initial supermatrices with full taxon sampling (12 species)

Supermatrices after selecting the 50 best genes with genesortR (12 species)

Removed the two species of Platyhelminthes (10 species in total)

Removed alignment columns with unique amino-acid residues in some or all species (10 species in total, see materials and methods)

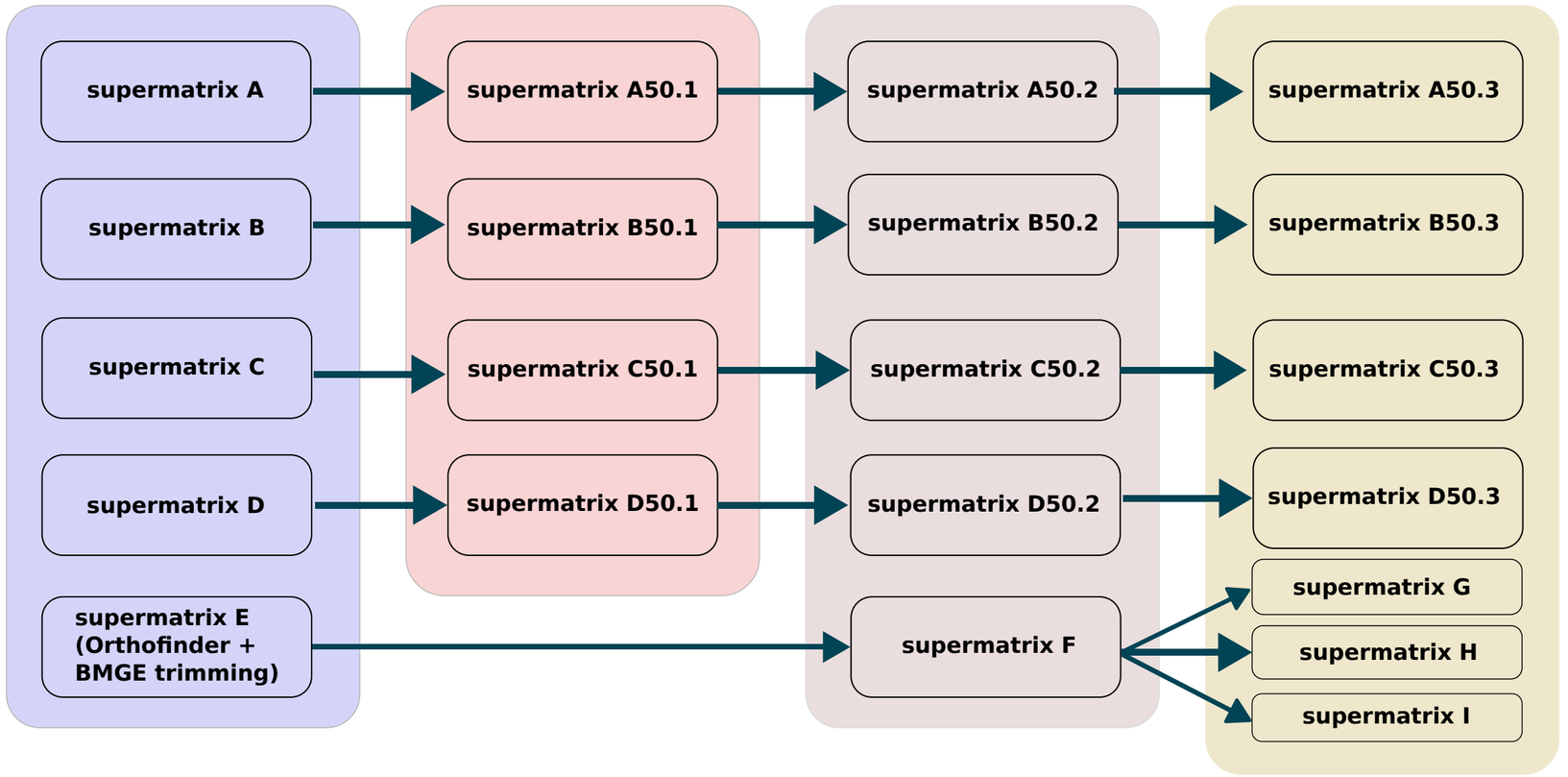

b)

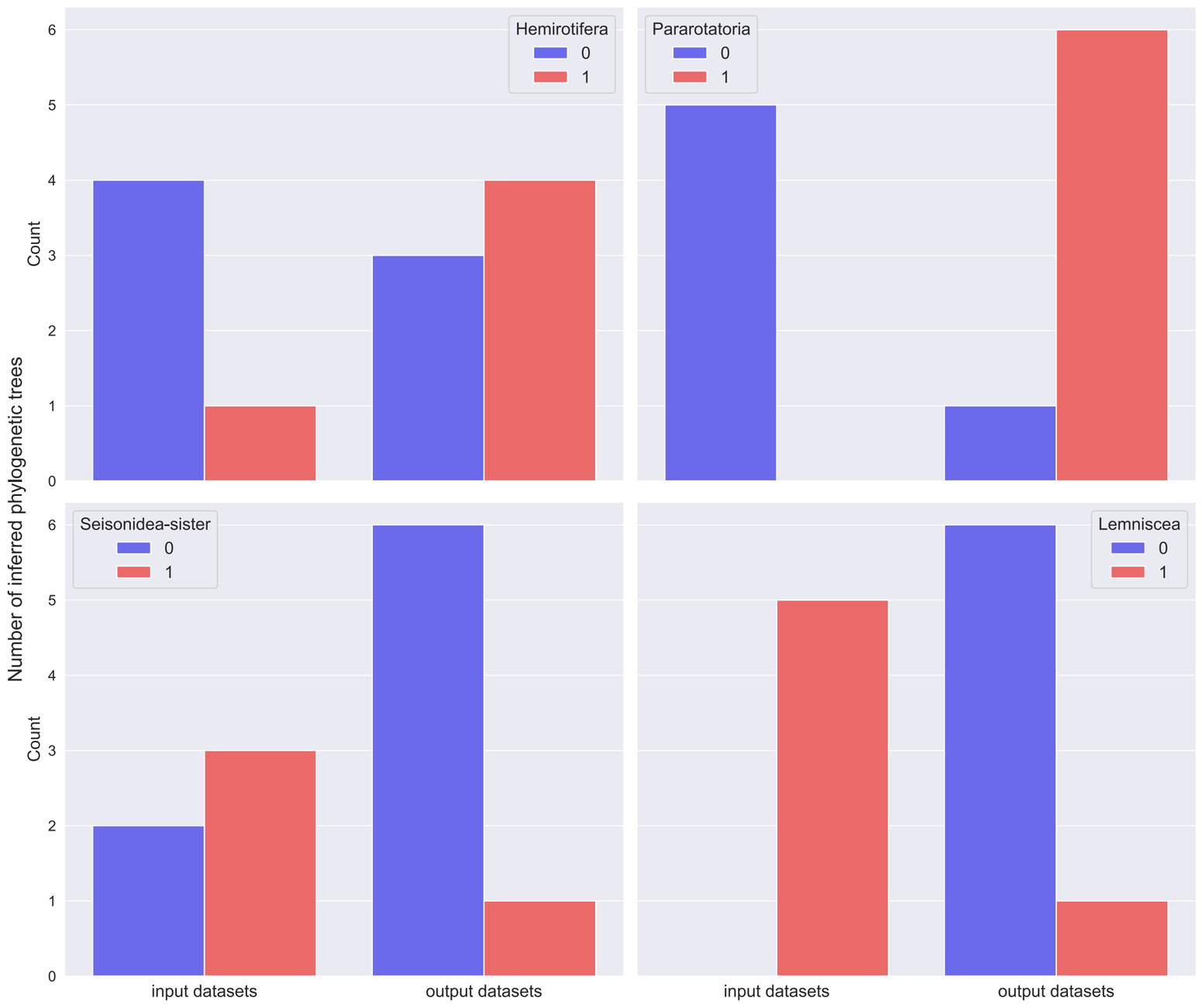

c)

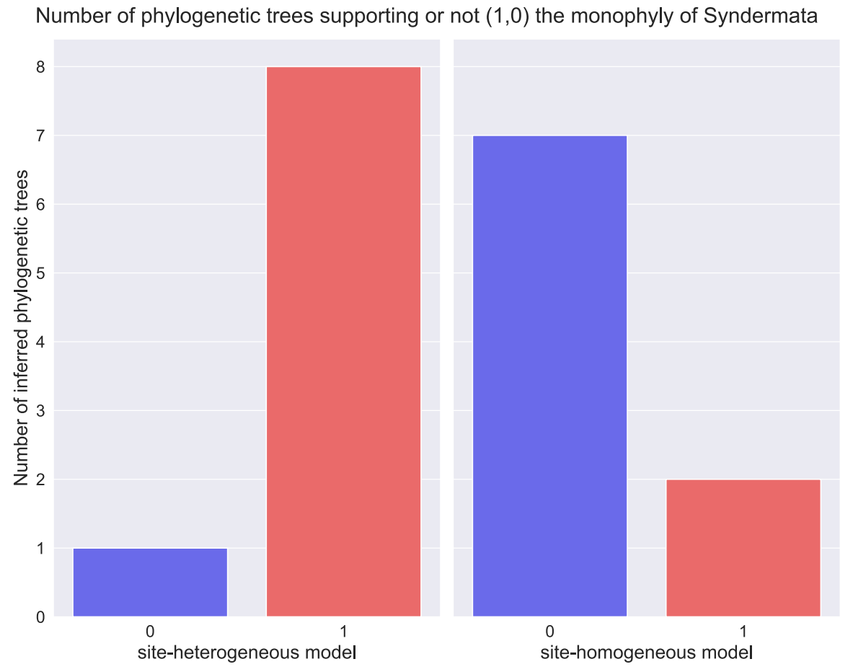

d)

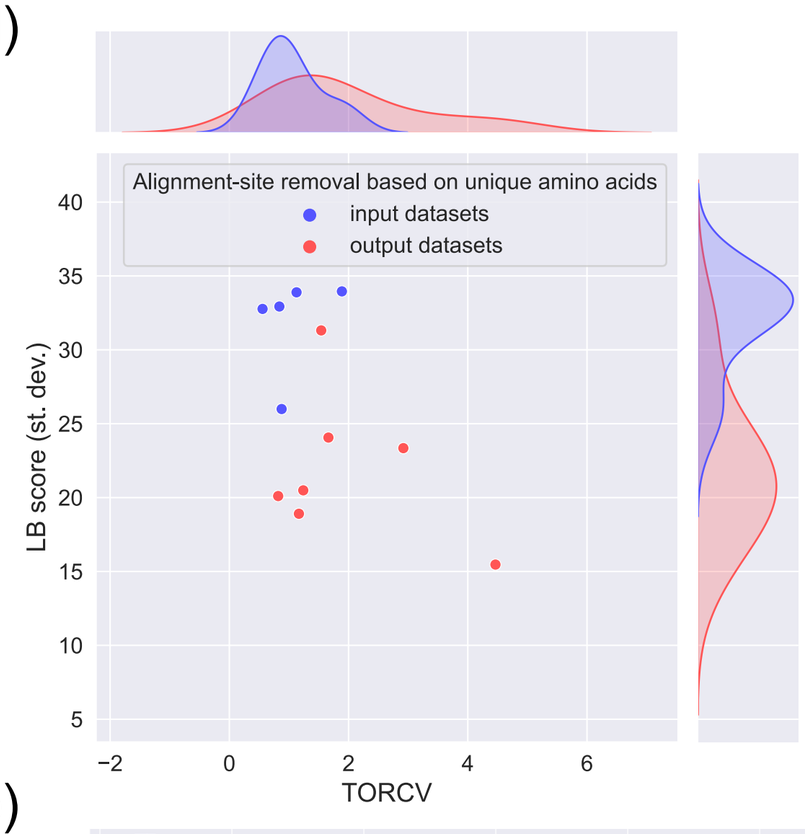

e)

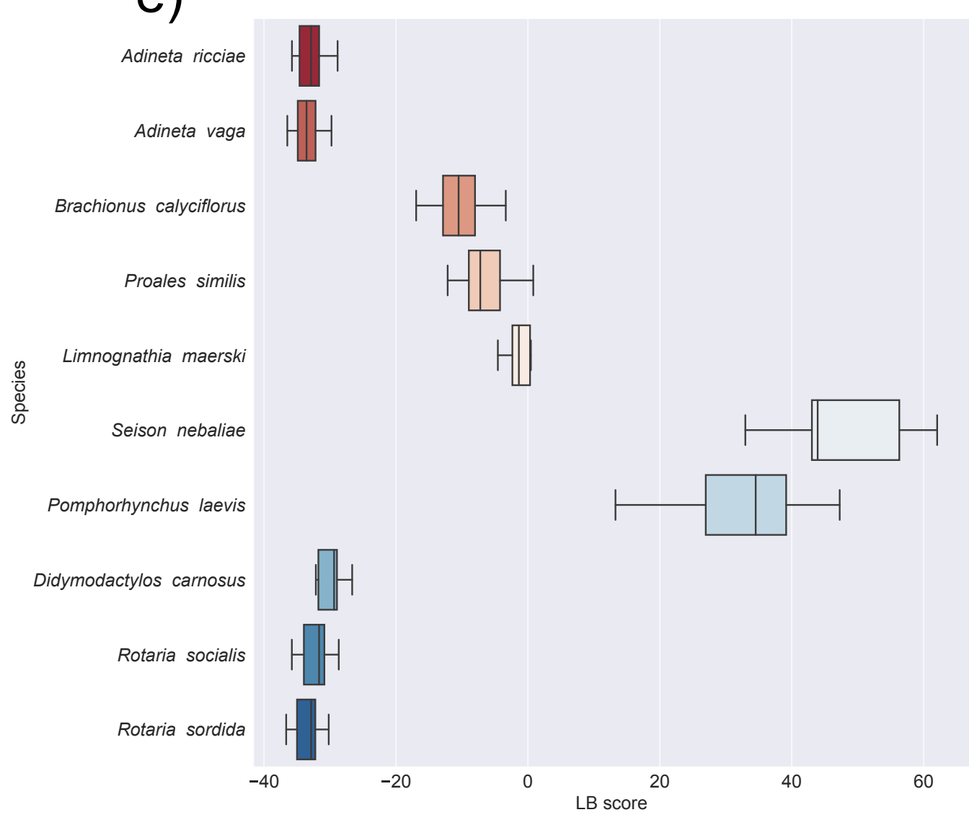

a)

Seisonidea-sister hypothesis

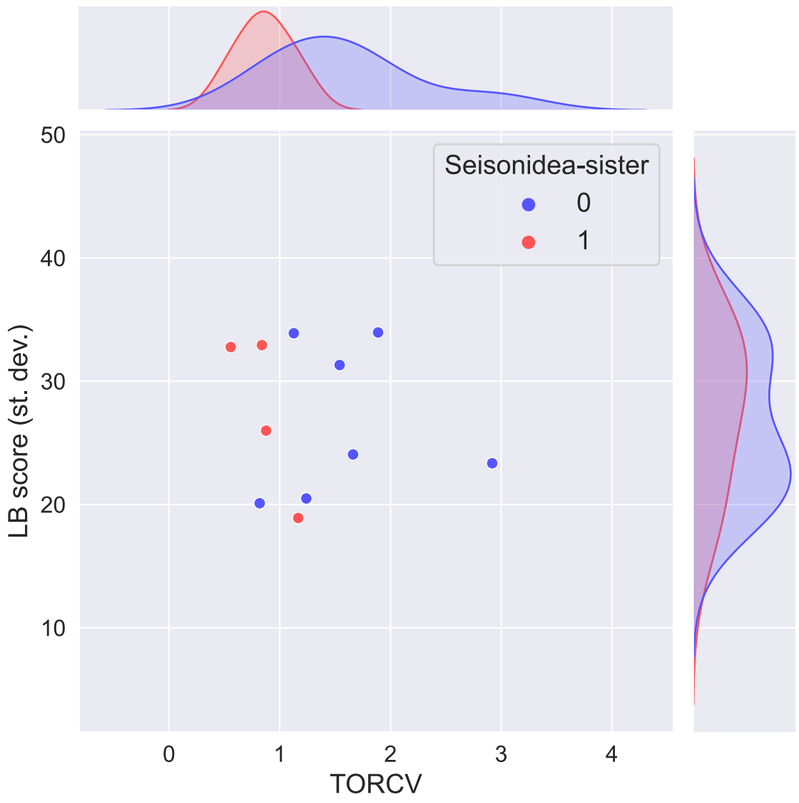

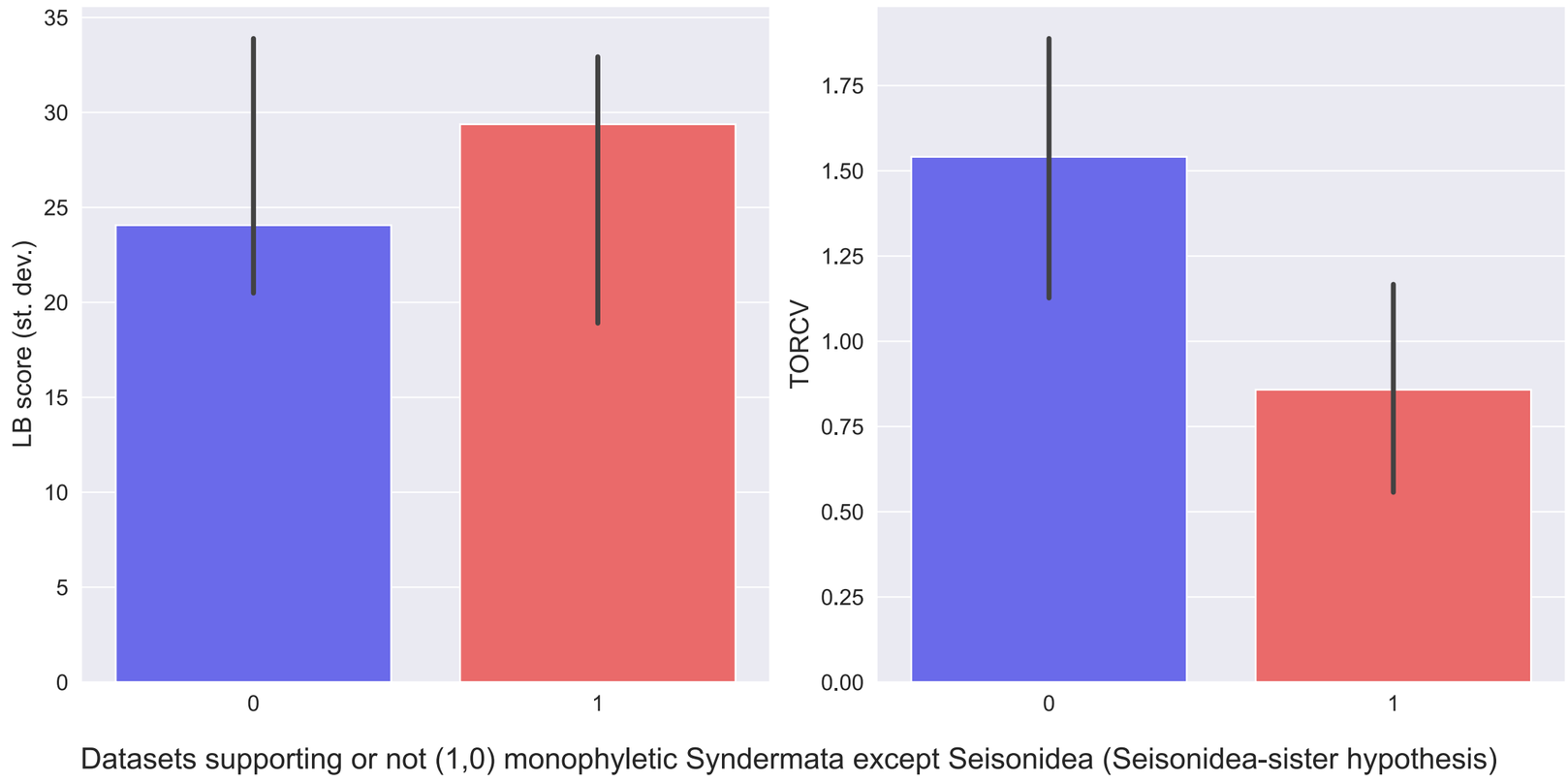

b)

Lemniscea hypothesis

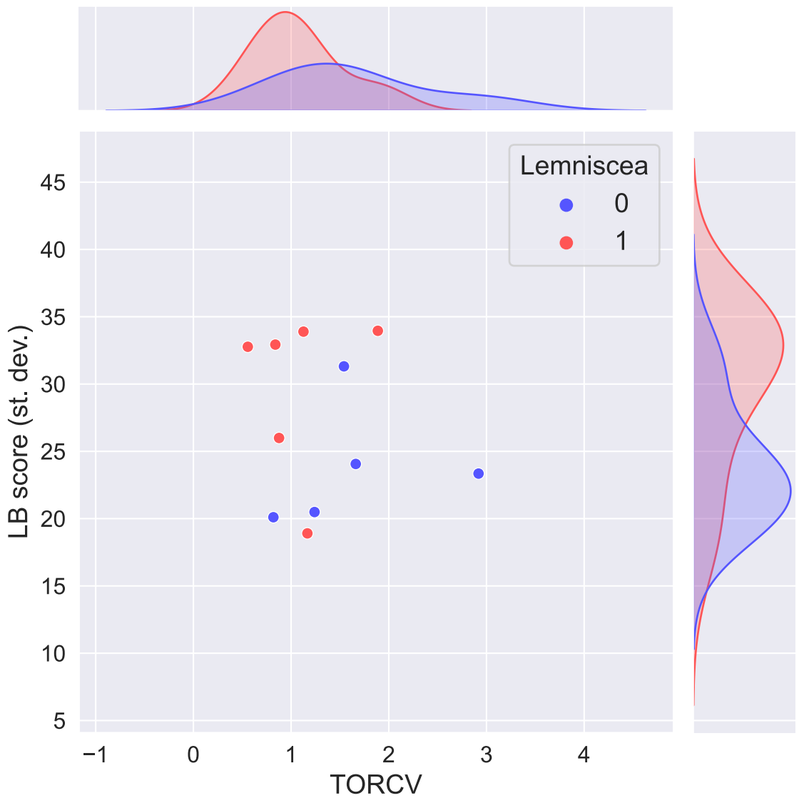

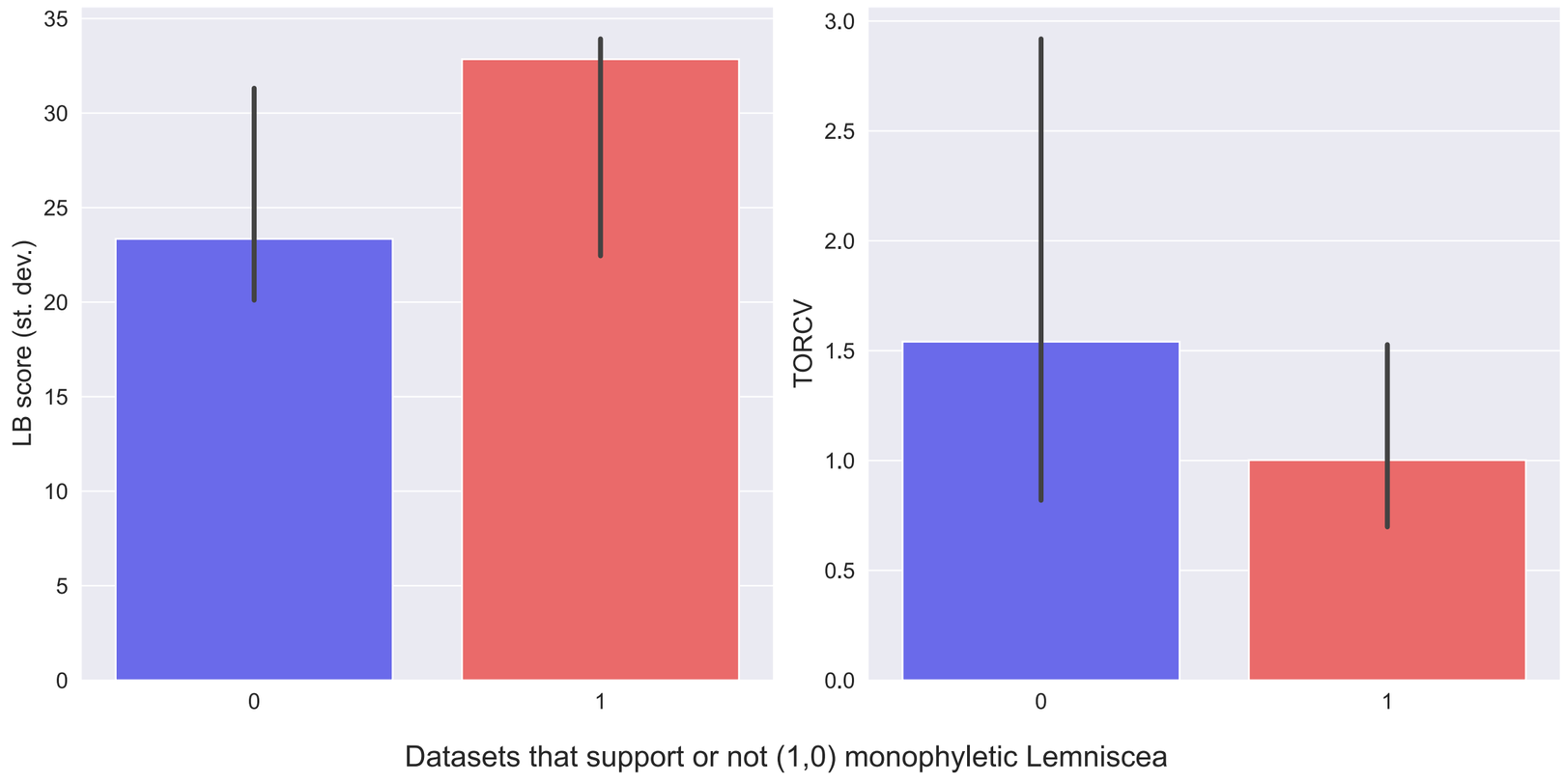

c)

Hemirotifera hypothesis

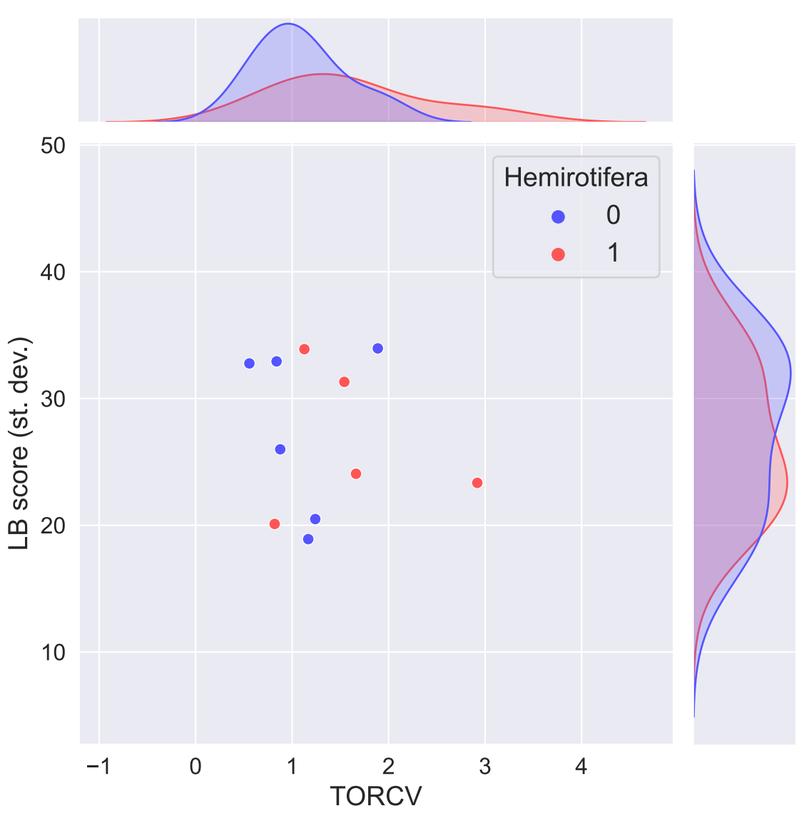

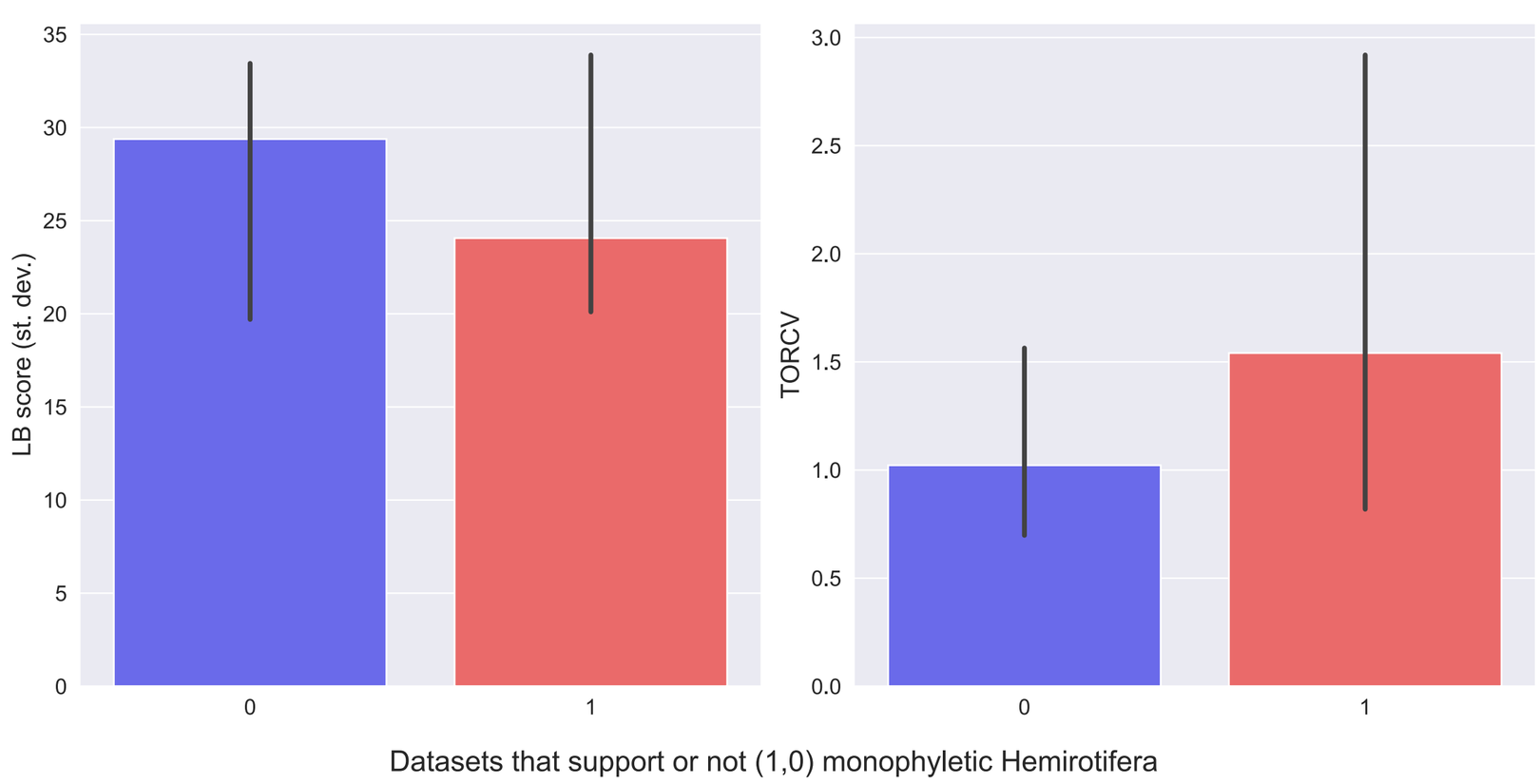

d)

Pararotatoria hypothesis

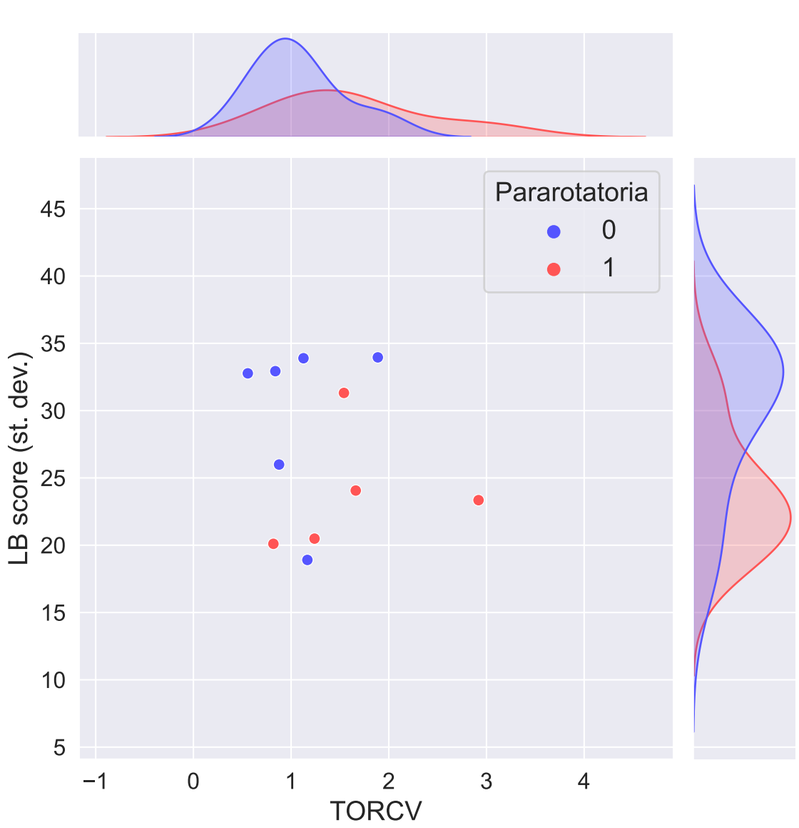

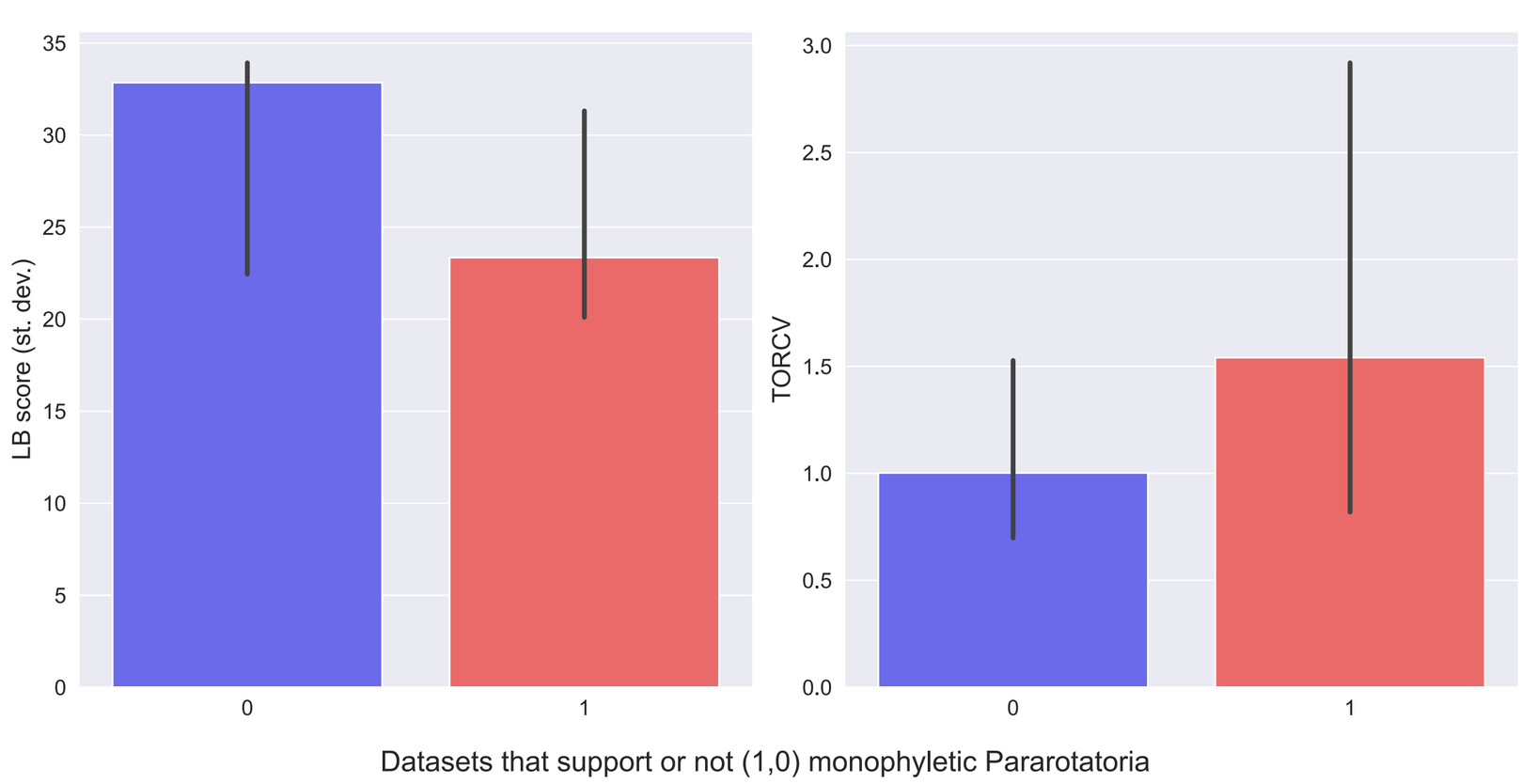

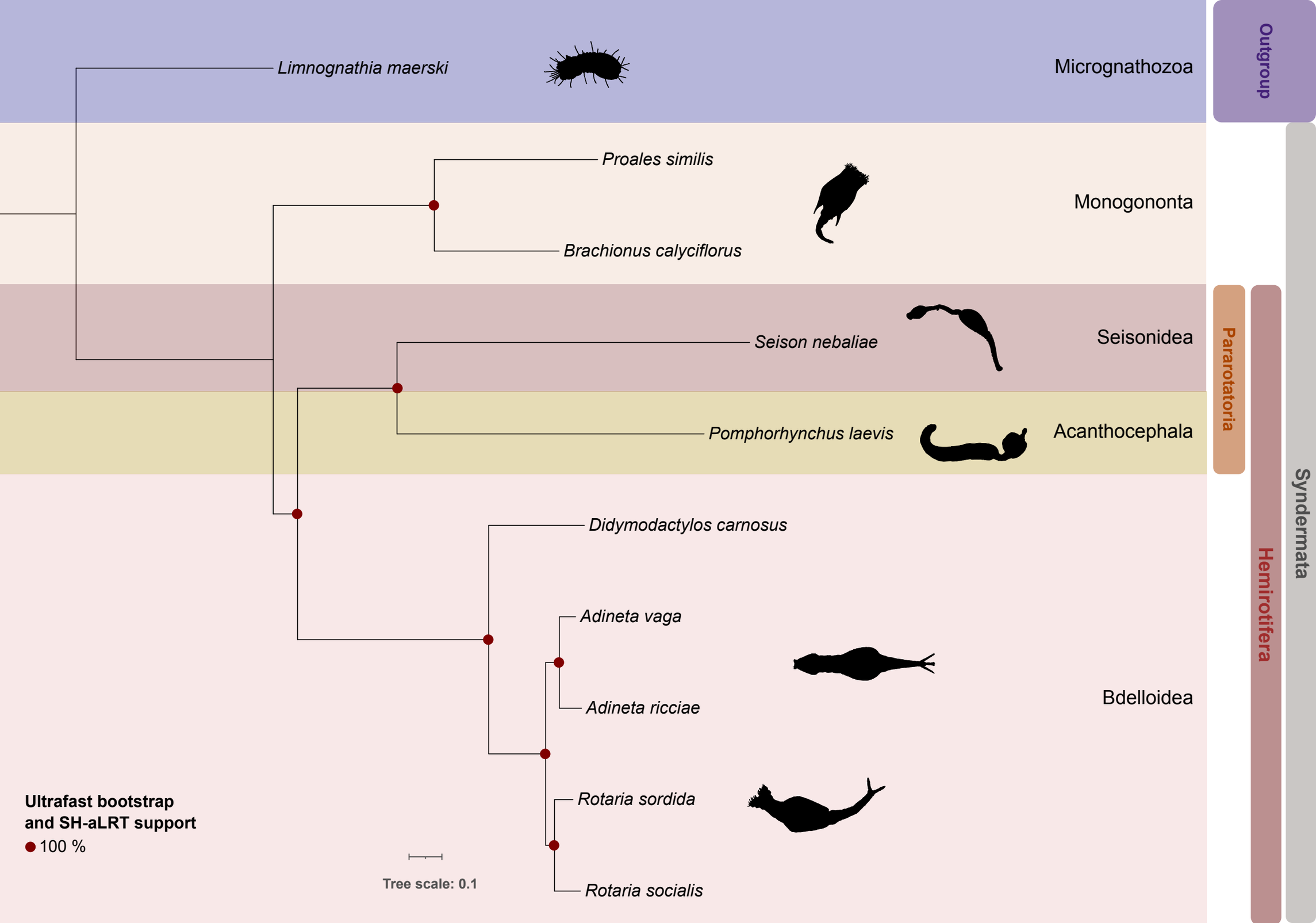
Limnognathia maerski
Micrognathozoa
Outgroup
Proales similis
Brachionus calyciflorus
Monogononta
Seison nebaliae
Seisonidea
Pararotatoria
Pomphorhynchus laevis
Acanthocephala
Hemirotifera
Syndermata
Didymodactylos carnosus
Adineta vaga
Adineta ricciae
Bdelloidea
Rotaria sordida
Rotaria socialis
Ultrafast bootstrap
and SH-aLRT support
100 %
Tree scale: 0.1

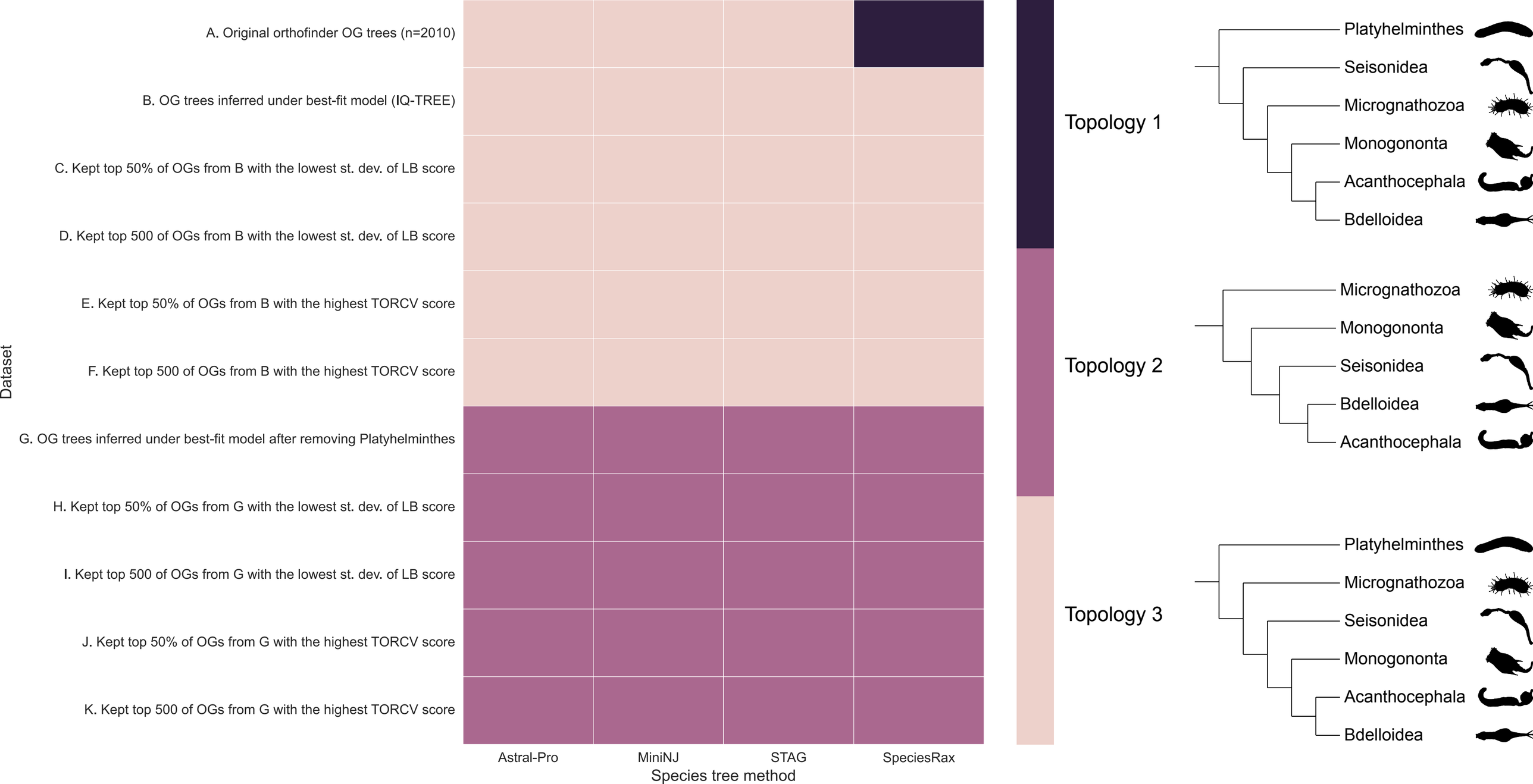
A. Original orthofinder OG trees (n=2010)
B. OG trees inferred under best-fit model (IQ-TREE)
C. Kept top 50% of OGs from B with the lowest st. dev. of LB score
D. Kept top 500 of OGs from B with the lowest st. dev. of LB score
E. Kept top 50% of OGs from B with the highest TORCV score
F. Kept top 500 of OGs from B with the highest TORCV score
G. OG trees inferred under best-fit model after removing Platyhelminthes
H. Kept top 50% of OGs from G with the lowest st. dev. of LB score
I. Kept top 500 of OGs from G with the lowest st. dev. of LB score
J. Kept top 50% of OGs from G with the highest TORCV score
K. Kept top 500 of OGs from G with the highest TORCV score
Dataset
Astral-Pro
MiniNJ
STAG
SpeciesRax
Species tree method
Topology 1
Platyhelminthes
Seisonidea
Micrognathozoa
Monogononta
Acanthocephala
Bdelloidea
Topology 2
Micrognathozoa
Monogononta
Seisonidea
Bdelloidea
Acanthocephala
Topology 3
Platyhelminthes
Micrognathozoa
Seisonidea
Monogononta
Acanthocephala
Bdelloidea

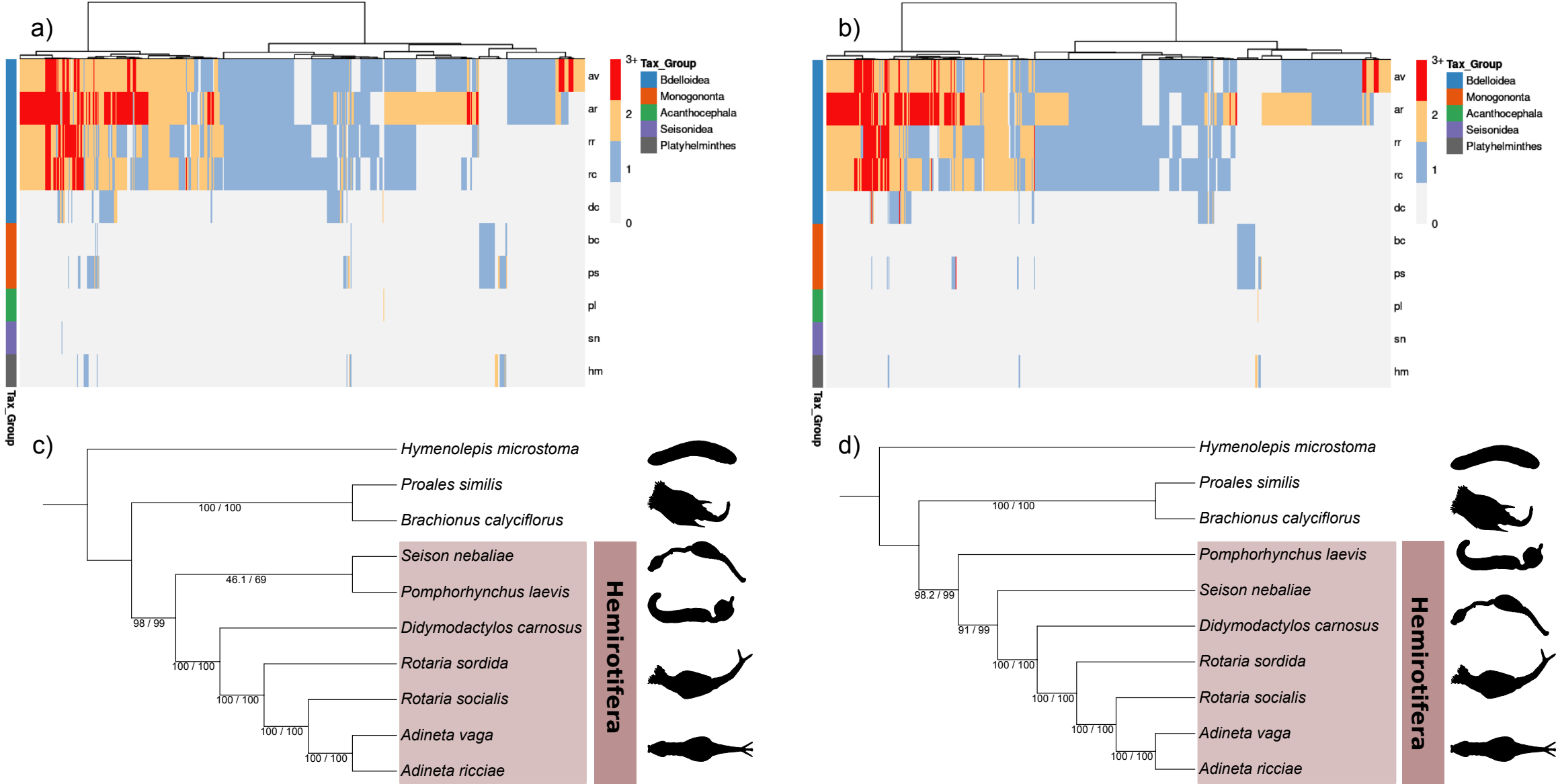
a)
b)
av
ar
rr
rc
dc
bc
ps
pl
sn
hm
Tax_Group
3+
2
1
0
Bdelloidea
Monogononta
Acanthocephala
Seisonidea
Platyhelminthes
c)
Hymenolepis microstoma
Proales similis
Brachionus calyciflorus
Seison nebaliae
Pomphorhynchus laevis
Didymodactylos carnosus
Rotaria sordida
Rotaria socialis
Adineta vaga
Adineta ricciae
100 / 100
46.1 / 69
98 / 99
100 / 100
100 / 100
100 / 100
100 / 100
Hemirotifera
d)
Hymenolepis microstoma
Proales similis
Brachionus calyciflorus
Pomphorhynchus laevis
Seison nebaliae
Didymodactylos carnosus
Rotaria sordida
Rotaria socialis
Adineta vaga
Adineta ricciae
100 / 100
98.2 / 99
91 / 99
100 / 100
100 / 100
100 / 100
100 / 100
Hemirotifera